

Chemistry–A European Journal

Supporting Information

Tuning the π -Accepting Properties of Mesoionic Carbenes: A Combined Computational and Experimental Study

Zhaowen Dong, J. Terence Blaskovits, Farzaneh Fadaei-Tirani, Rosario Scopelliti,
Andrzej Sienkiewicz, Clémence Corminboeuf,* and Kay Severin*

Table of Contents

| | |
|----------------------------------|------------|
| Experimental Details | S2 |
| EPR Measurements | S21 |
| Crystallographic Analyses | S23 |
| Computational Details | S30 |
| References | S36 |

Experimental Details

General. All reactions were performed under a controlled dry nitrogen atmosphere using a high-vacuum line, standard Schlenk techniques, and an MBraun glovebox. The used glassware was dried in an oven at 130 °C and evacuated prior to use. The solvents THF, diethyl ether (Et₂O), benzene, acetonitrile (MeCN), and *n*-pentane were dried by using an innovation technology SPS solvent system. Deuterated dichloromethane (CD₂Cl₂) was dried by storing over molecular sieve (4 Å) for at least one day before degassing by three freeze-pump-thaw cycles. Standard chemicals were obtained from commercial suppliers and used as delivered if not mentioned otherwise. The N-heterocyclic carbene IDipp was synthesized according to a literature procedure.^[1]

NMR spectroscopy. NMR spectra were recorded on Bruker AVANCE DPX-400 and AVANCE IIIHD-600 spectrometers. ¹H NMR spectra were calibrated against the residual proton signal of the solvent as internal reference (CD₂Cl₂: δ¹H(CDHCl₂) = 5.32; C₆D₆: δ¹H(C₆H₅D) = 7.16) and ¹³C {¹H} NMR spectra by using the central line of the solvent signal (CD₂Cl₂: δ¹³C(CDHCl₂) = 53.8; C₆D₆: δ¹³C(C₆H₅D) = 128.1).

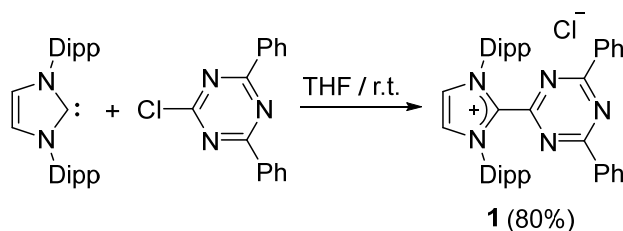
Mass spectrometry: High-resolution mass spectra were recorded on an LTQ Orbitrap ELITE ETD with a nanoESI source or a Xevo G2-S QTOF with an ESI source. Combustion analysis was performed with a Thermo Scientific Flash 2000 Organic Elemental Analyzer.

EPR spectroscopy: The EPR measurements were performed at room temperature using a Bruker EleXsys E500 X-band EPR spectrometer, which was equipped with a high-Q cylindrical cavity, Model ER 4122 SHQE (from Bruker BioSpin GmbH, Karlsruhe, Germany).

UV-vis and UV-vis-NIR spectroscopy: Data were recorded on a Cary 60 Spectrometer (Agilent Technologies) and a Shimadzu 3600 Plus UV-Vis-NIR Spectrophotometer.

IR Spectroscopy: The IR measurements were carried out using a neat CH₂Cl₂ solution (c. 0.1mM) on a PerkinElmer UATR Two Spectrometer

Synthesis of imidazolium salt **1**:



Scheme S1.

THF (40 mL) was added to a mixture of IDipp (3.0 g, 7.726 mmol) and 2-chloro-4,6-diphenyl-1,3,5-triazine (2.1 g, 7.726 mmol) at room temperature. The resulting suspension was stirred overnight. Subsequently, the solvent was removed under reduced pressure, and the resulting white solid was washed three times with *n*-pentane (3 x 15 mL). Colorless crystals of **1** were obtained by recrystallization from MeCN at -40 °C after one day (Yield: 4.1 g, 80%).

^1H NMR (400 MHz, 298 K, CD_2Cl_2): δ = 0.95 (d, $^3J(^1\text{H}-^1\text{H})$ = 6.8 Hz, 12H, $\text{CH}(\underline{\text{C}}\text{H}_3)_2$), 1.33 (d, $^3J(^1\text{H}-^1\text{H})$ = 6.8 Hz, 12H, $\text{CH}(\underline{\text{C}}\text{H}_3)_2$), 2.49 (sept., $^3J(^1\text{H}-^1\text{H})$ = 6.8 Hz, 4H, $\underline{\text{C}}\text{H}(\text{CH}_3)_2$), 7.37 (m, 4H, Ph), 7.53 (d, $^3J(^1\text{H}-^1\text{H})$ = 7.9 Hz, 4H, *m*-Dipp), 7.59 (m, 2H, *p*-Ph), 7.67 (m, 4H, Ph), 7.78 (t, $^3J(^1\text{H}-^1\text{H})$ = 8.0 Hz, 2H, *p*-Dipp), 8.92 (s, 2H, N- $\underline{\text{C}}\text{H}=\text{CH}$).

$^{13}\text{C}\{^1\text{H}\}$ NMR (101 MHz, 298 K, CD_2Cl_2): δ = 23.1, 24.5 ($\text{CH}(\underline{\text{C}}\text{H}_3)_2$), 29.9 ($\underline{\text{C}}\text{H}(\text{CH}_3)_2$), 125.6 (*m*-Dipp), 129.0, 129.6 (*m*, *o*-Ph), 131.0 ($\underline{\text{C}}\text{H}=\text{CH}$), 131.7 (*p*-Dipp), 133.7 (*ipso*-Dipp), 133.9 (*ipso*-Ph), 134.6 (*p*-Ph), 138.2 (N- $\underline{\text{C}}-\text{N}$), 144.0 (*o*-Dipp), 159.8 (NHC- $\underline{\text{C}}\text{N}_2$), 172.7 (Ph- $\underline{\text{C}}\text{N}_2$).

HRMS (nanochip-ESI/LTQ-Orbitrap) *m/z*: $[\text{M}]^+$ Calcd for $\text{C}_{42}\text{H}_{46}\text{N}_5^+$ 620.3748; Found 620.3739.

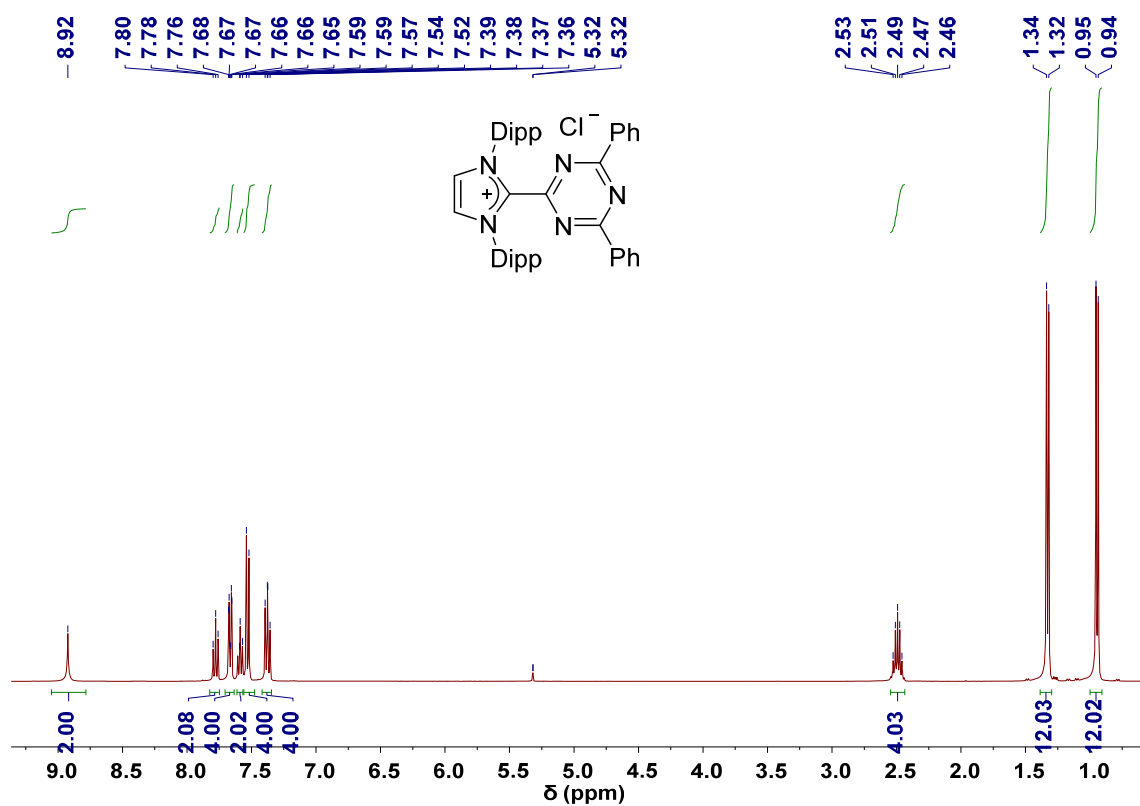


Figure S1a. $^1\text{H NMR}$ (400 MHz, 298 K, CD_2Cl_2) spectrum of imidazolium salt 1.

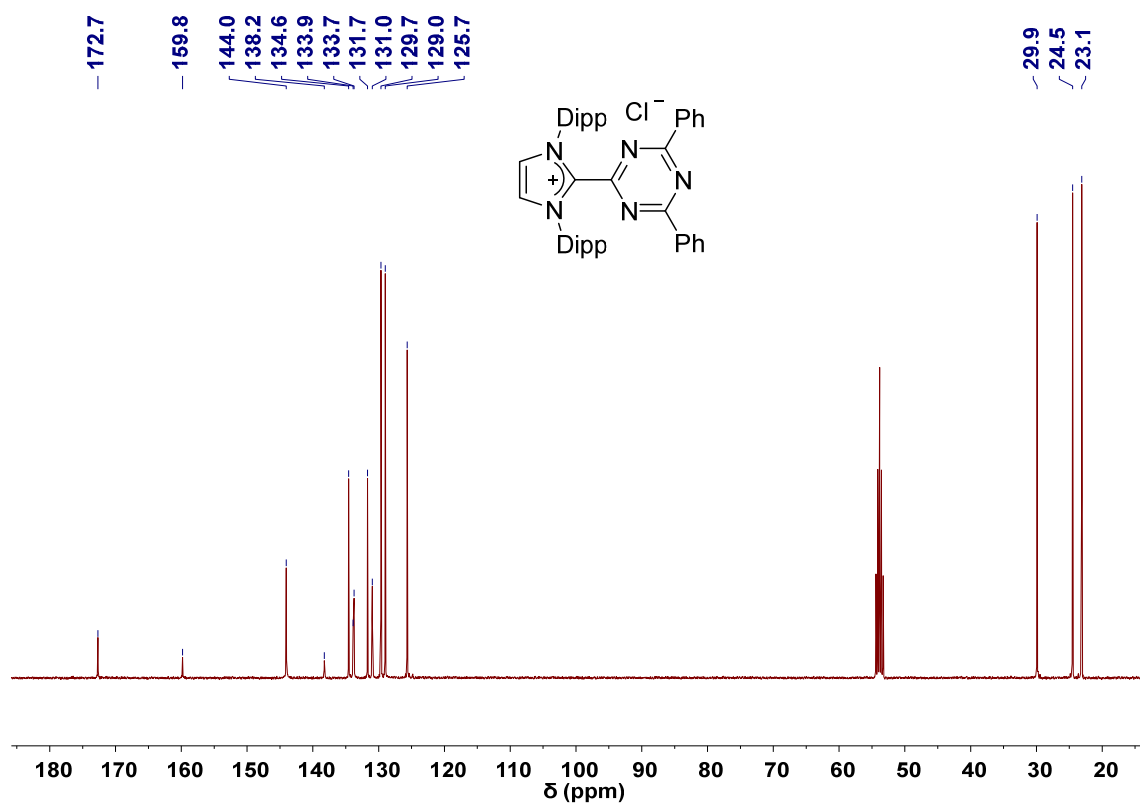


Figure S1b. $^{13}\text{C}\{^1\text{H}\}$ NMR (101 MHz, 298 K, CD_2Cl_2) spectrum of imidazolium salt 1.

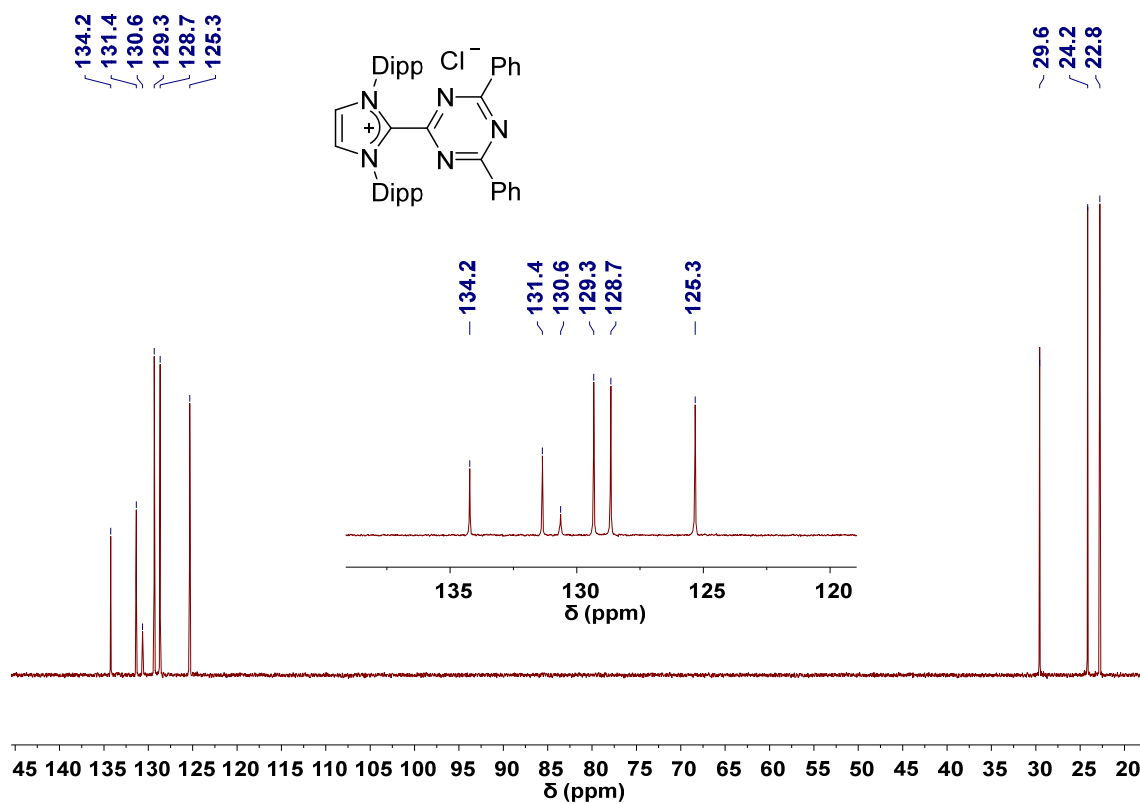


Figure S1c. ^{13}C DEPT NMR (101 MHz, 298 K, CD_2Cl_2) spectrum of imidazolium salt 1.

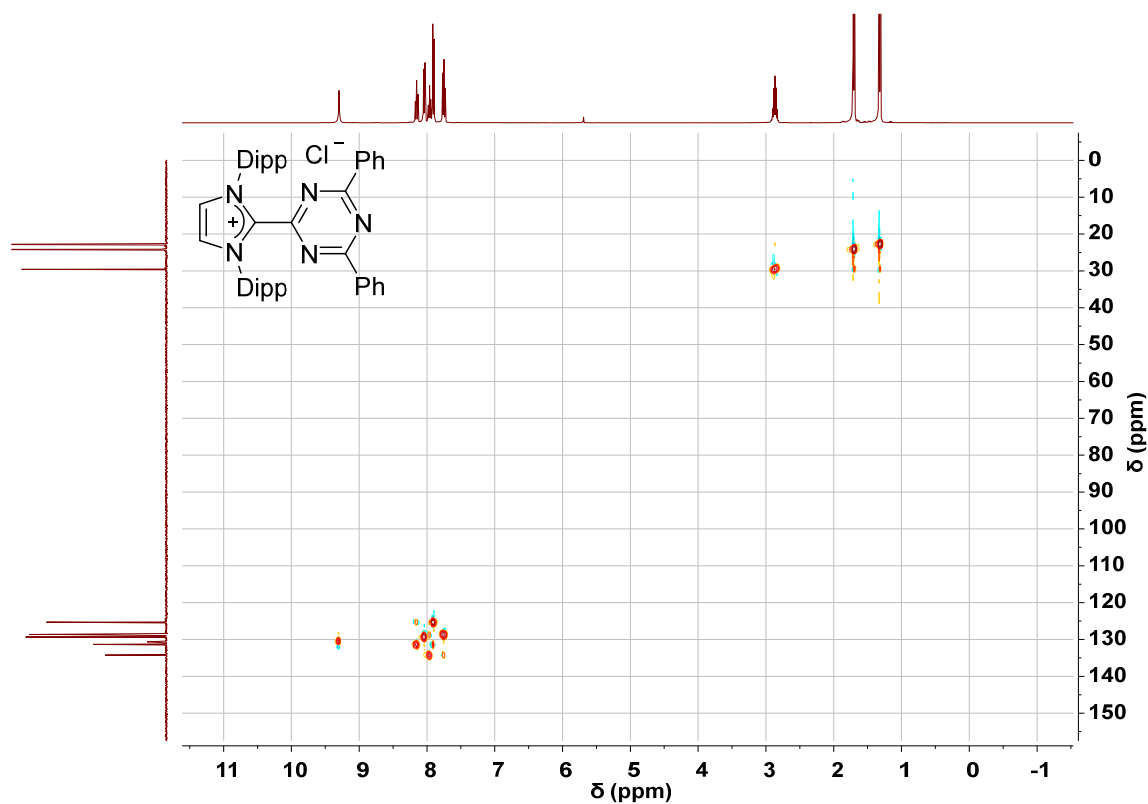


Figure S1d. $^1\text{H}^{13}\text{C}$ HSQC NMR (298 K, CD_2Cl_2) spectrum of imidazolium salt 1.

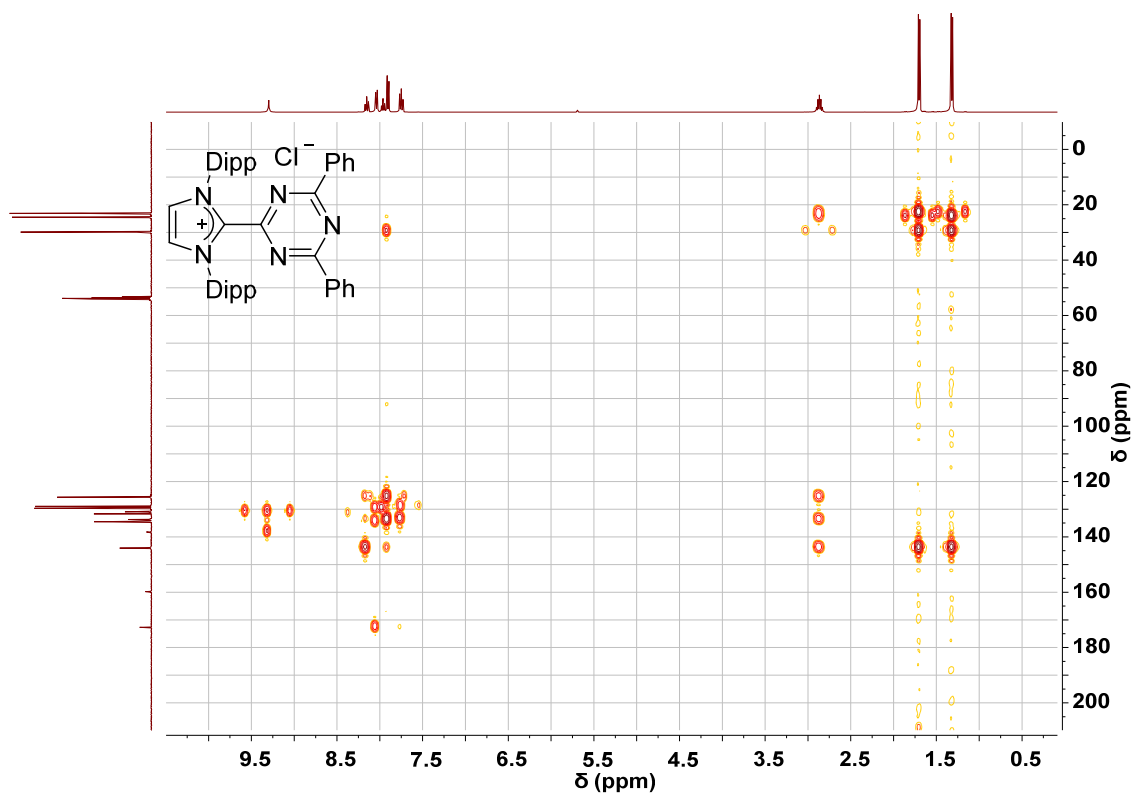
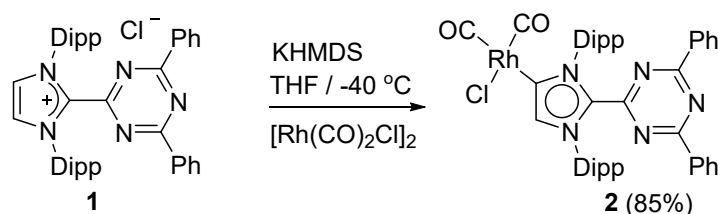


Figure S1e. ^1H ^{13}C HMBC NMR (298 K, CD_2Cl_2) spectrum of imidazolium salt **1**.

Synthesis of rhodium complex **2**:



Scheme S2.

KHMDS (32 mg, 0.160 mmol) was added to a stirred THF solution (10 ml) of imidazolium salt **1** (100 mg, 0.152 mmol) at -40 °C. The color of the solution changed immediately to orange. After 2 min, [Rh(CO)₂Cl]₂ (30 mg, 0.077 mmol) was added to the reaction mixture. Then the solution was allowed to stir overnight. Subsequently, the solvent was removed under reduced pressure, and the resulting red-brown solid was extracted with *n*-pentane / Et₂O (2:1, 15 ml). The red solution was filtered by using a PTFE syringe filter to remove the KCl. The filtrate was concentrated to 5 mL and stored at -40 °C for two days. Clear red crystals of **2**, suitable for single crystal XRD analysis, were obtained (Yield: 106 mg, 85%).

¹H NMR (400 MHz, 298 K, CD₂Cl₂): δ = 0.87 (d, ³*J*(¹H-¹H) = 6.9 Hz, 6H, CH(CH₃)₂), 0.92 (d, ³*J*(¹H-¹H) = 6.9 Hz, 6H, CH(CH₃)₂), 1.29 (d, ³*J*(¹H-¹H) = 6.9 Hz, 6H, CH(CH₃)₂), 1.43 (d, ³*J*(¹H-¹H) = 6.9 Hz, 6H, CH(CH₃)₂), 2.55 (sept., ³*J*(¹H-¹H) = 6.9 Hz, 2H, CH(CH₃)₂), 2.74 (sept., ³*J*(¹H-¹H) = 6.9 Hz, 2H, CH(CH₃)₂), 7.36 (m, 4H, *m*-Ph), 7.47 (d, ³*J*(¹H-¹H) = 7.9 Hz, 2H, *m*-Dipp), 7.48 (d, ³*J*(¹H-¹H) = 7.9 Hz, 2H, *m*-Dipp), 7.55 (m, 2H, *p*-Ph), 7.67 (m, 4H, *o*-Ph), 7.69 (m, 1H, *p*-Dipp), 7.71 (m, 1H, *p*-Dipp), 7.89 (s, 1H, NCH).

¹³C{¹H} NMR (101 MHz, 298 K, CD₂Cl₂): δ = 23.1, 23.6, 24.0, 24.6 (CH(CH₃)₂), 29.5, 29.6 (CH(CH₃)₂), 125.2, 125.3 (*m*-Dipp), 128.7 (*m*-Ph), 129.6 (*o*-Ph), 130.5, 130.6 (*p*-Dipp), 133.8 (*p*-Ph), 134.6 (*ipso*-Ph), 135.5, 139.3 (*ipso*-Dipp), 136.0 (N-CH), 138.2 (N-C-N), 144.2, 144.9 (*o*-Dipp), 160.4 (NHC-CN₂), 168.3 (C_{carbene}-Rh, d, ¹*J*_{C-Rh} = 44 Hz), 172.0 (Ph-CN₂), 183.2 (CO_{cis}, d, ¹*J*_{C-Rh} = 76 Hz), 186.7 (CO_{trans}, d, ¹*J*_{C-Rh} = 52 Hz).

HRMS (standard-ESI/LTQ-Orbitrap) *m/z*: [M-Cl]⁺ Calcd for C₄₄H₄₅N₅O₂Rh⁺ 778.2623; Found 778.2605.

Elemental analysis (%): Calcd for C₄₄H₄₅ClN₅O₂Rh: C, 64.91; H, 5.57; N, 8.60. Found: C, 65.61; H, 5.95; N, 7.94.

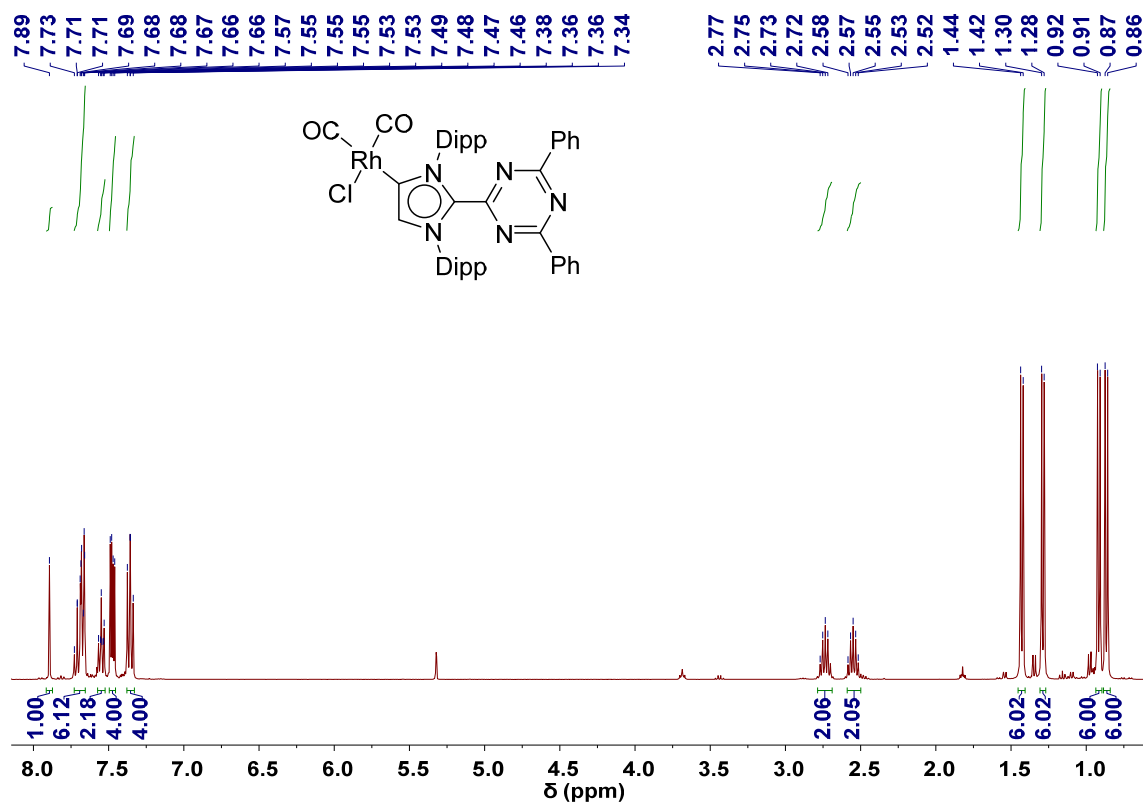


Figure S2a. $^1\text{H NMR}$ (400 MHz, 298 K, CD_2Cl_2) spectrum of rhodium complex 2.

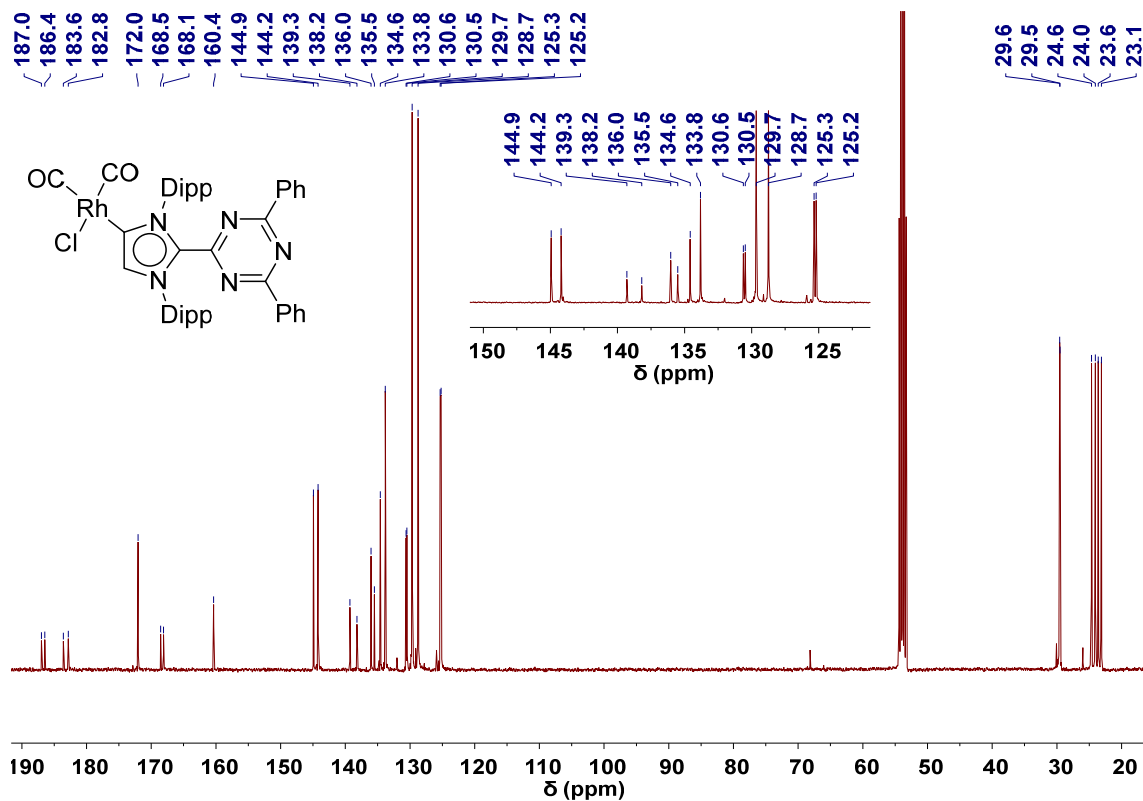
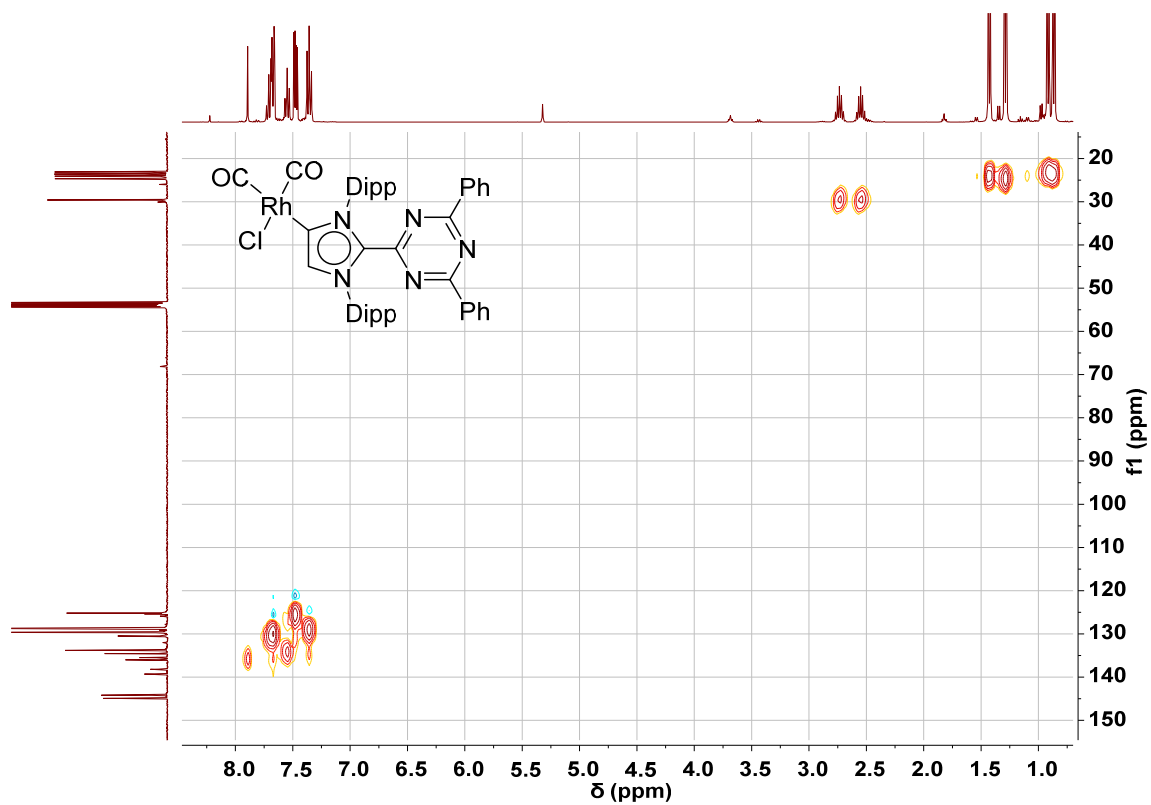
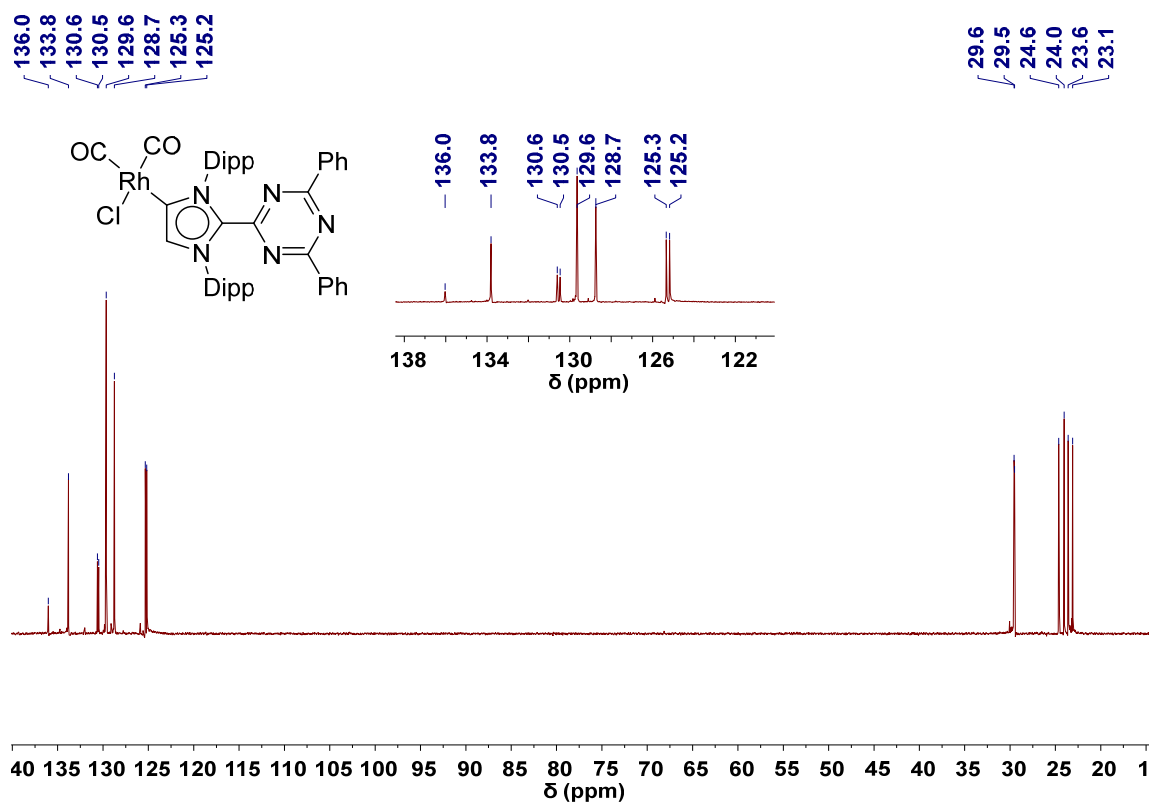


Figure S2b. $^{13}\text{C}\{^1\text{H}\}$ NMR (101 MHz, 298 K, CD_2Cl_2) spectrum of rhodium complex 2.



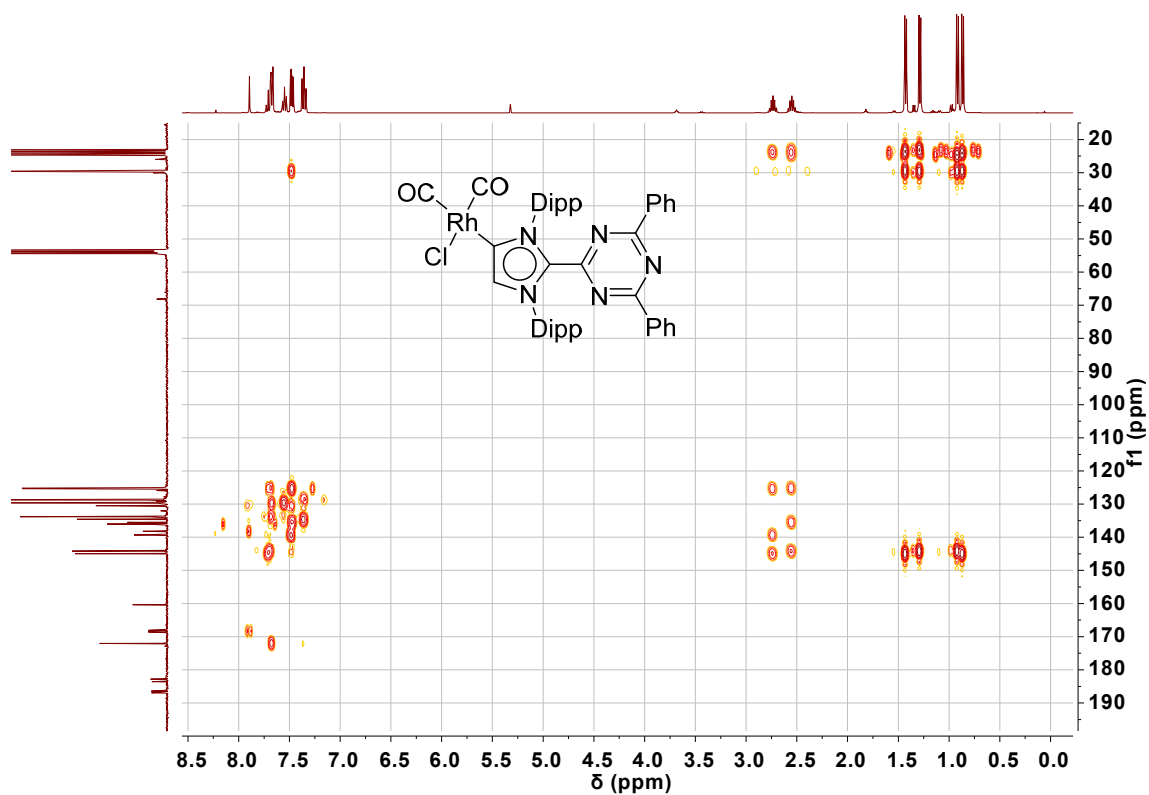


Figure S2e. ^{13}C HMBC NMR (298 K, CD_2Cl_2) spectrum of rhodium complex **2**.

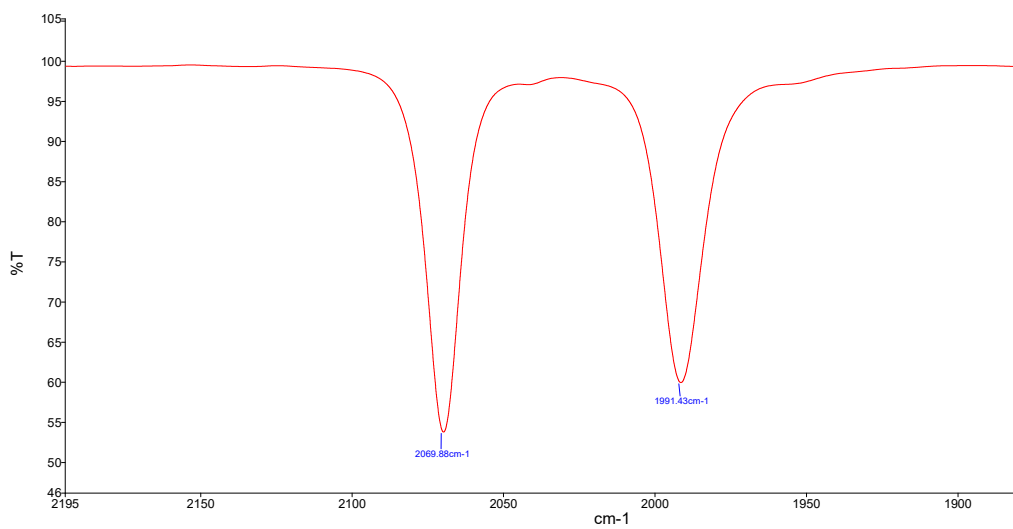
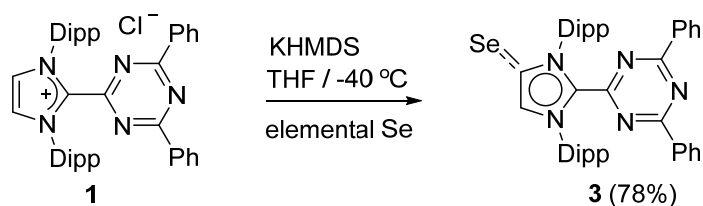


Figure S2f. CO region of the IR spectrum of the carbonyl rhodium complex **2** (in DCM). The CO bands appear at $\nu(\text{CO})_{\text{avg.}} = 2031 \text{ cm}^{-1}$.

Synthesis of selenium adduct **3**:



Scheme S3.

KHMDS (31 mg, 0.155 mmol) was added to a stirred THF solution (10 ml) of imidazolium salt **1** (100 mg, 0.152 mmol) at $-40\text{ }^{\circ}\text{C}$. After 2 min, elemental Se (24 mg, 0.304 mmol) was added to the reaction mixture. The color of the solution changed immediately to deep blue. Then the solution was allowed to stir overnight. The solvent was removed under reduced pressure, and the resulting blue solid was extracted with *n*-pentane / Et₂O (2:1, 15 ml). The blue solution was filtered by using a PTFE syringe filter to remove the KCl. The filtrate was concentrated to 5 mL and stored at $-40\text{ }^{\circ}\text{C}$ for one day. Clear intense blue crystals of **3**, suitable for single crystal XRD analysis, were obtained (Yield: 83 mg, 78%).

¹H NMR (600 MHz, 298 K, C₆D₆): δ = 0.78 (d, ³*J*(¹H-¹H) = 6.9 Hz, 6H, CH(CH₃)₂), 0.93 (d, ³*J*(¹H-¹H) = 6.9 Hz, 6H, CH(CH₃)₂), 0.98 (d, ³*J*(¹H-¹H) = 6.9 Hz, 6H, CH(CH₃)₂), 1.61 (d, ³*J*(¹H-¹H) = 6.9 Hz, 6H, CH(CH₃)₂), 2.74 (sept., ³*J*(¹H-¹H) = 6.9 Hz, 2H, CH(CH₃)₂), 3.05 (sept., ³*J*(¹H-¹H) = 6.9 Hz, 2H, CH(CH₃)₂), 7.05 (d, ³*J*(¹H-¹H) = 7.9 Hz, 2H, *m*-Dipp), 7.06 (s, 1H, NCH), 7.12 (m, 4H, Ph), 7.21 (m, 2H, *p*-Ph), 7.27 (m, 1H, *p*-Dipp), 7.36 (d, ³*J*(¹H-¹H) = 7.9 Hz, 2H, *m*-Dipp), 7.49 (m, 1H, *p*-Dipp), 7.74 (m, 4H, Ph).

¹³C{¹H} NMR (151 MHz, 298 K, C₆D₆): δ = 23.1, 23.5, 24.0, 24.1 (CH(CH₃)₂), 29.3, 30.2 (CH(CH₃)₂), 124.8, 124.9 (*m*-Dipp), 128.5, 129.6 (*m*, *o*-Ph), 129.6, 129.9 (*p*-Dipp), 130.6 (N-CH), 133.3 (*p*-Ph), 133.8 (N-C-N), 135.0 (*ipso*-Ph), 135.7, 136.9 (*ipso*-Dipp), 143.9, 145.2 (*o*-Dipp), 155.0 (C_{carbene}-Se, ¹*J*_{C-Se} = 224 Hz), 158.4 (NHC-CN₂), 171.6 (Ph-CN₂).

⁷⁷Se{¹H} NMR (95 MHz, 298 K, C₆D₆): δ = 146.2

HRMS (standard-ESI/LTQ-Orbitrap) *m/z*: [M]⁺ Calcd for C₄₂H₄₅N₅Se⁺ 699.2835; Found 699.2836.

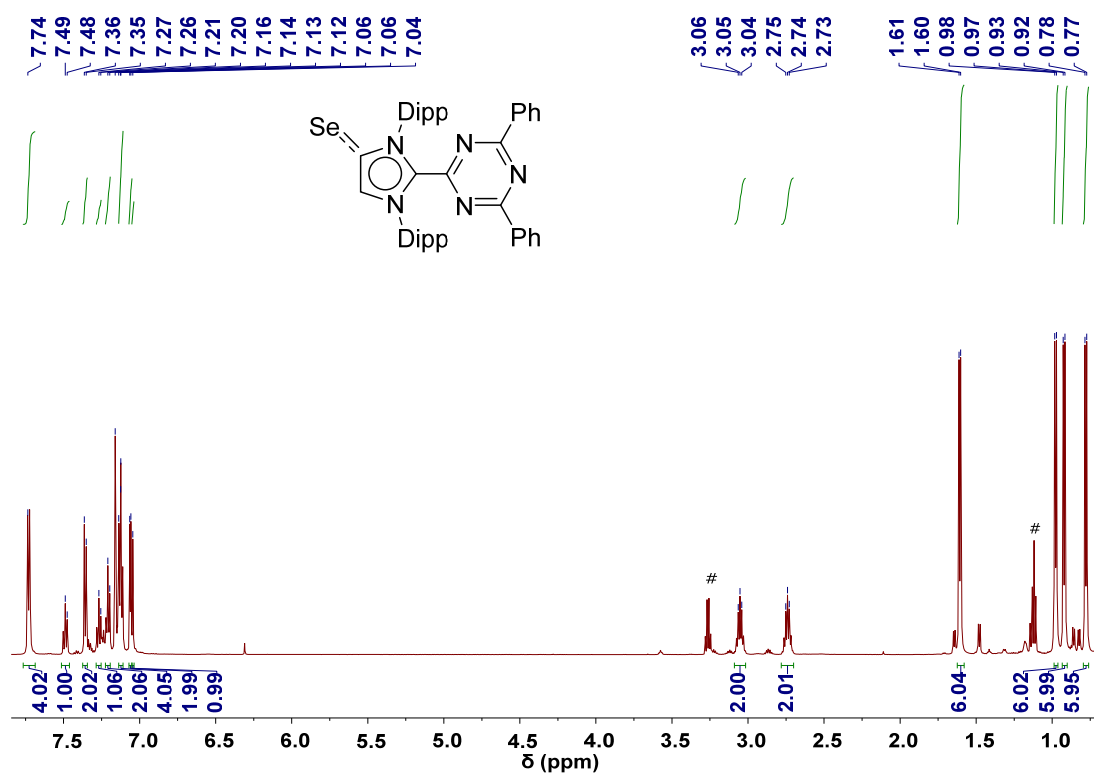


Figure S3a. ¹H NMR (600 MHz, 298 K, C₆D₆) spectrum of selenium adduct **3** (#: Et₂O). The NMR data point to the presence of minor amounts of side products, which could not be separated.

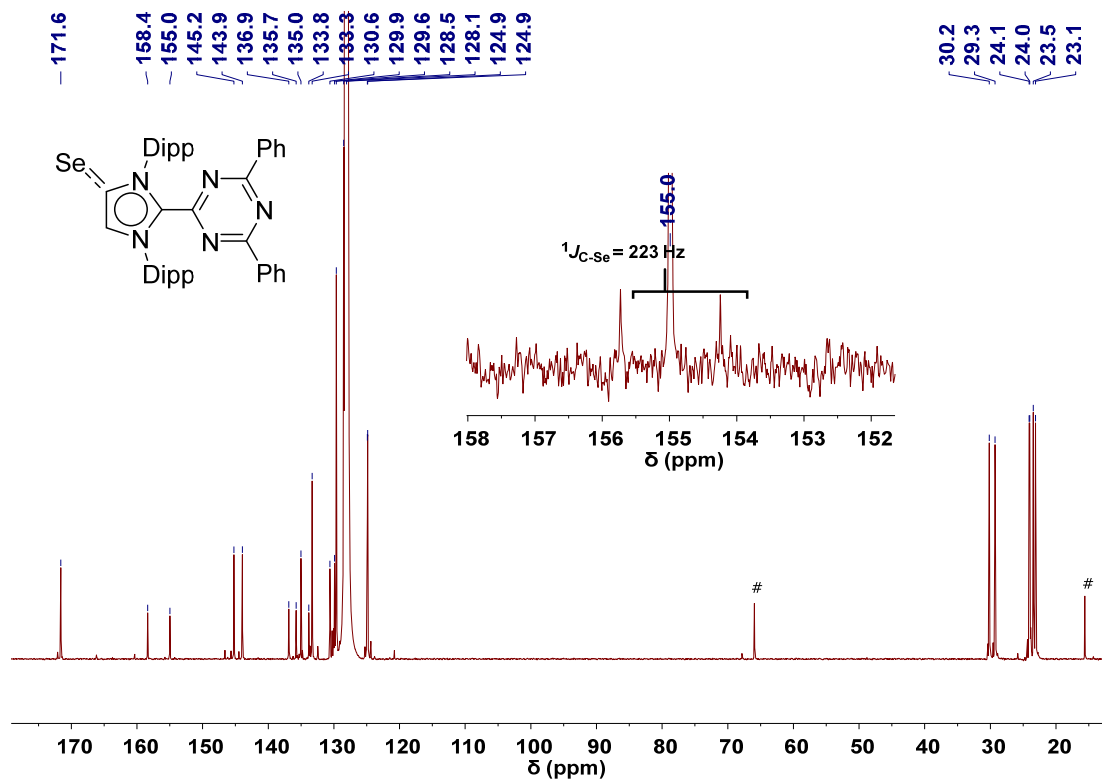


Figure S3b. ¹³C{¹H} NMR (151 MHz, 298 K, C₆D₆) spectrum of selenium adduct **3** (#: Et₂O).

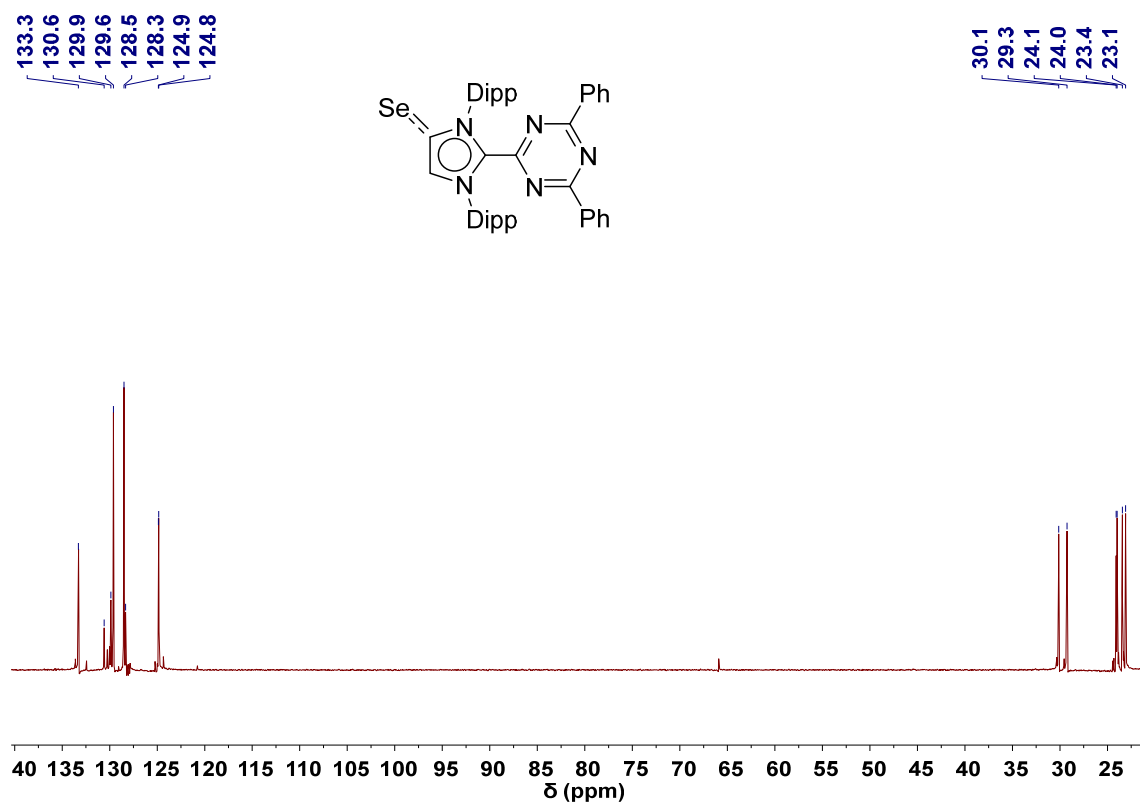


Figure S3c. ¹³C DEPT NMR (151 MHz, 298 K, C₆D₆) spectrum of selenium adduct **3**.

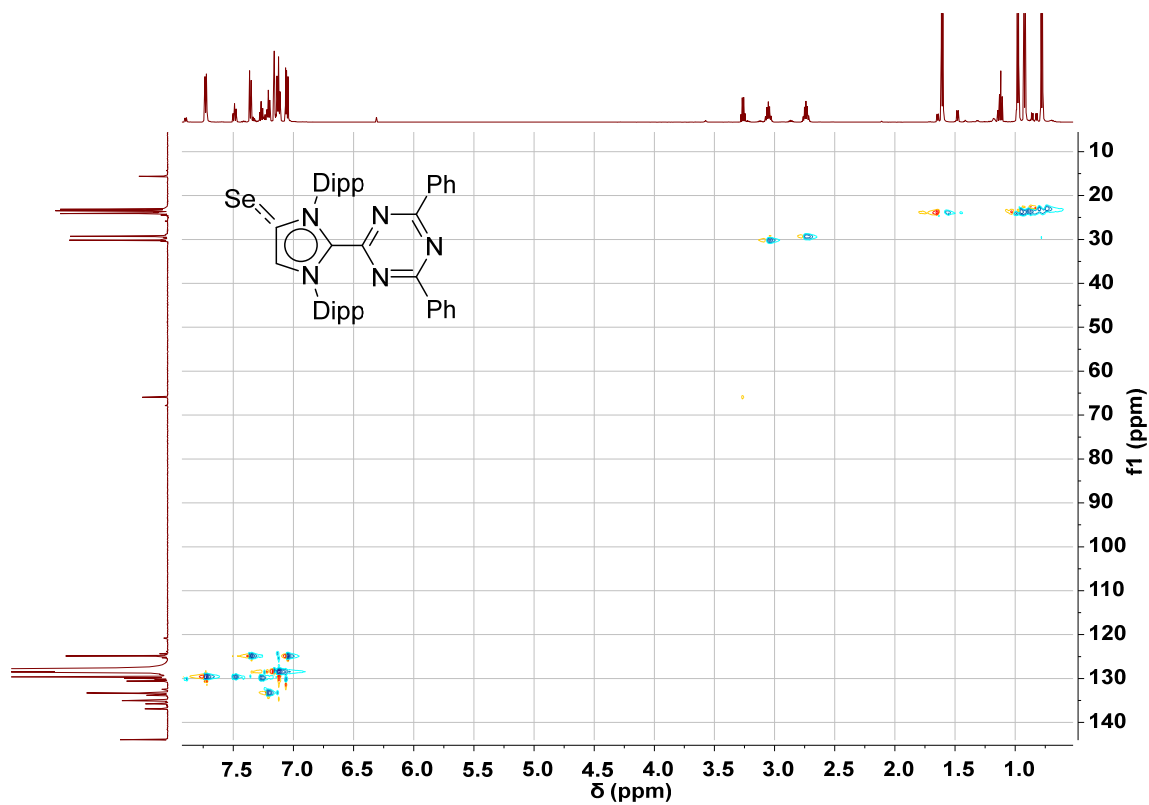


Figure S3d. ¹H¹³C HSQC NMR (298 K, C₆D₆) spectrum of selenium adduct **3**.

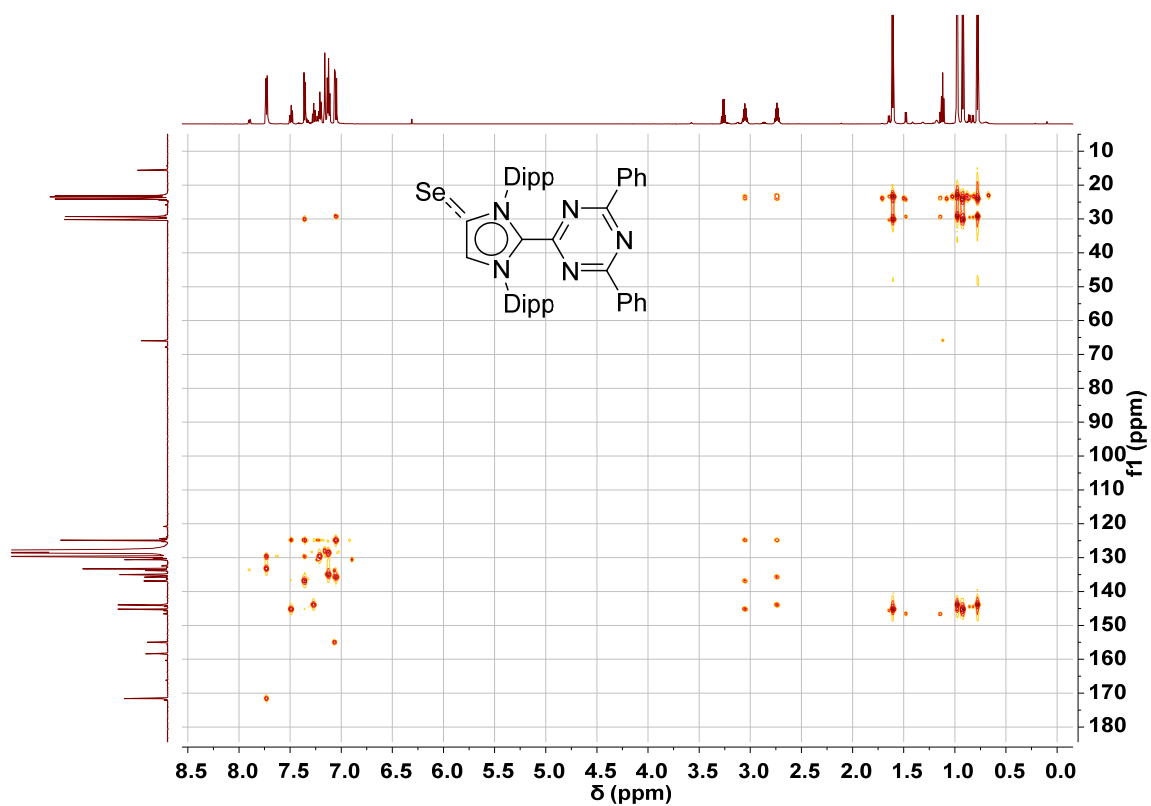


Figure S3e. $^1\text{H}^{13}\text{C}$ HMBC NMR (298 K, C_6D_6) spectrum of selenium adduct **3**.

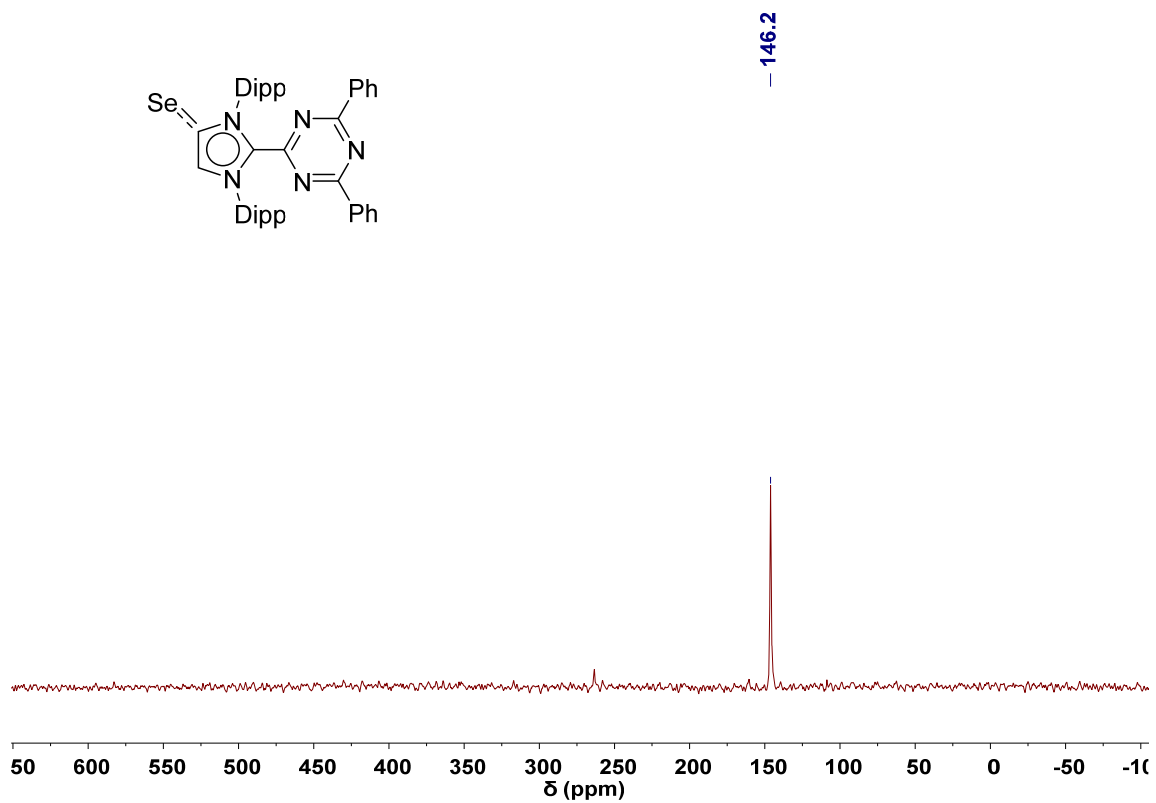
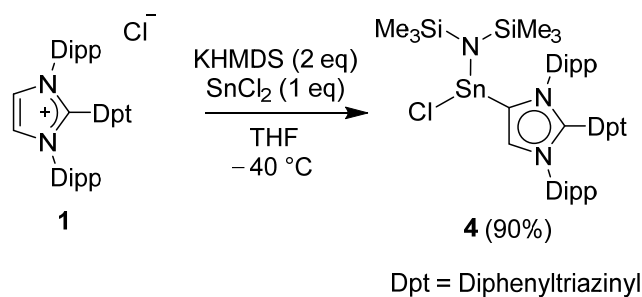


Figure S3f. $^{77}\text{Se}\{^1\text{H}\}$ NMR (95 MHz, 298 K, C_6D_6) spectrum of selenium adduct **3**.

Synthesis of stannylene 4:



Scheme S4.

KHMDS (62 mg, 0.312 mmol) was added to a stirred THF solution (6 ml) of imidazolium salt **1** (100 mg, 0.152 mmol) at $-40\text{ }^{\circ}\text{C}$. The color of the solution changed immediately to orange. After 15 min, anhydrous SnCl_2 (29 mg, 0.152 mmol), was added to the reaction mixture. Then the solution was allowed to stir overnight. Subsequently, the solvent was removed under reduced pressure, and the resulting orange solid was extracted with *n*-pentane / THF (3:1, 15 ml). The orange solution was filtered by using a PTFE syringe filter to remove the KCl. The filtrate was concentrated to $\sim 5\text{ mL}$ and stored at $-40\text{ }^{\circ}\text{C}$ for one day. Clear yellow crystals of **4**, suitable for XRD analysis, were obtained (Yield: 128 mg, 90%).

^1H NMR (400 MHz, 298 K, THF-d_8): $\delta = 0.08$ (s, SiMe_3), 0.84, 0.86 (d, $^3J(\text{H}-\text{H}) = 6.6\text{ Hz}$, 6H, $\text{CH}(\text{CH}_3)_2$), 0.94, 0.95 (d, $^3J(\text{H}-\text{H}) = 6.5\text{ Hz}$, 6H, $\text{CH}(\text{CH}_3)_2$), 1.30 (d, $^3J(\text{H}-\text{H}) = 7.0\text{ Hz}$, 6H, $\text{CH}(\text{CH}_3)_2$), 1.44, 1.46 (d, $^3J(\text{H}-\text{H}) = 7.9\text{ Hz}$, 6H, $\text{CH}(\text{CH}_3)_2$), 2.61 (sept., $^3J(\text{H}-\text{H}) = 6.9\text{ Hz}$, 2H, $\text{CH}(\text{CH}_3)_2$), 2.71 (sept., $^3J(\text{H}-\text{H}) = 6.9\text{ Hz}$, 1H, $\text{CH}(\text{CH}_3)_2$), 2.85 (sept., $^3J(\text{H}-\text{H}) = 6.9\text{ Hz}$, 1H, $\text{CH}(\text{CH}_3)_2$), 7.37 (m, 4H, *m*-Ph), 7.57 (m, 6H, *m*-Dipp, *p*-Ph), 7.70 (m, 4H, *o*-Ph), 7.75 (m, 2H, *p*-Dipp), 7.88 (s, 1H, NCH).

$^{13}\text{C}\{^1\text{H}\}$ NMR (101 MHz, 298 K, THF-d_8): $\delta = 6.7$ (SiMe_3), 23.1, 23.6, 24.1, 24.5, 24.9 ($\text{CH}(\text{CH}_3)_2$), 29.7, 29.8, 29.9, 30.0 ($\text{CH}(\text{CH}_3)_2$), 125.8, 125.9 (*m*-Dipp), 121.7 (*m*-Ph), 130.0 (*o*-Ph), 131.0, 131.2 (*p*-Dipp), 134.4 (*p*-Ph), 134.7 (*ipso*-Ph), 135.7, 137.2 (*ipso*-Dipp), 136.2 (N-CH), 139.6 (N-C-N), 144.3, 144.4, 144.6 (*o*-Dipp), 160.8 (NHC-CN₂), 172.6 (Ph-CN₂), 176.1 (C_{carbene}-Sn).

^{119}Sn NMR (149 MHz, 298 K, THF-d_8): $\delta = -31.6$ (s, SnCl).

HRMS (standard-ESI/LTQ-Orbitrap) *m/z*: $[\text{M}]^+$ Calcd for $\text{C}_{48}\text{H}_{63}\text{ClN}_6\text{Si}_2\text{Sn}^+$ 934.3363; Found 934.3547.

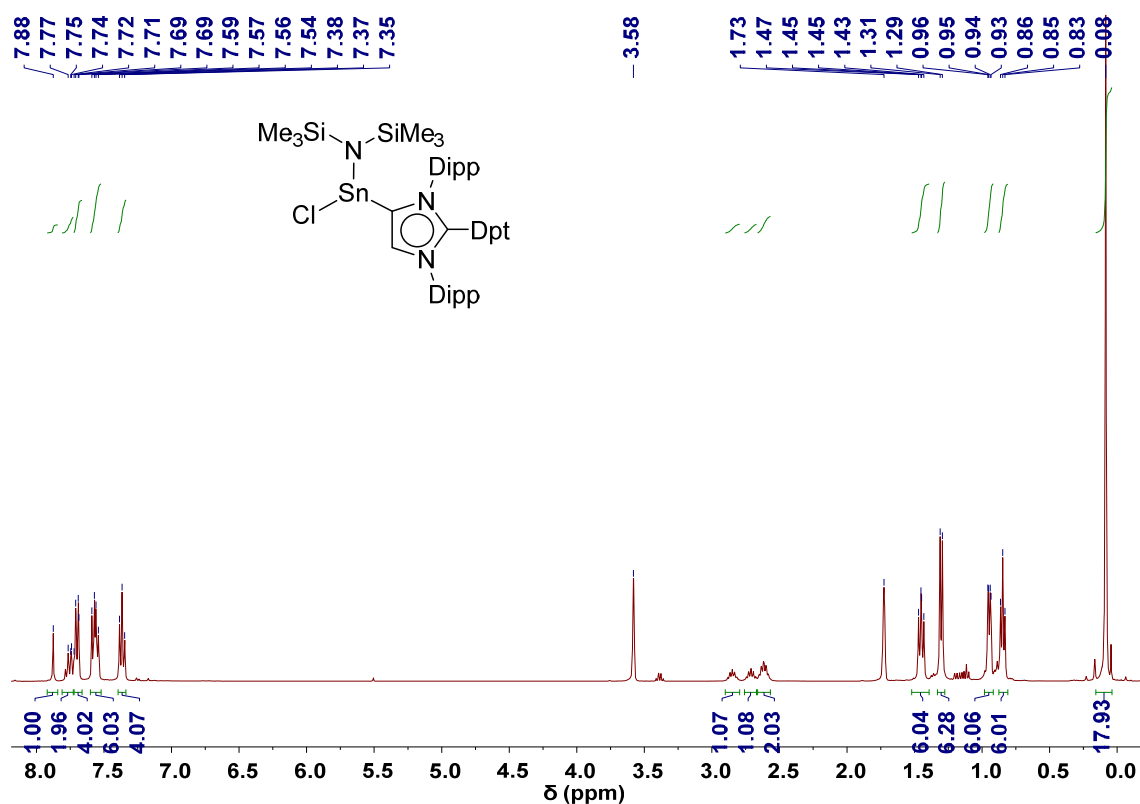


Figure S4a. $^1\text{H NMR}$ (400 MHz, 298 K, THF- d_8) spectrum of compound 4.

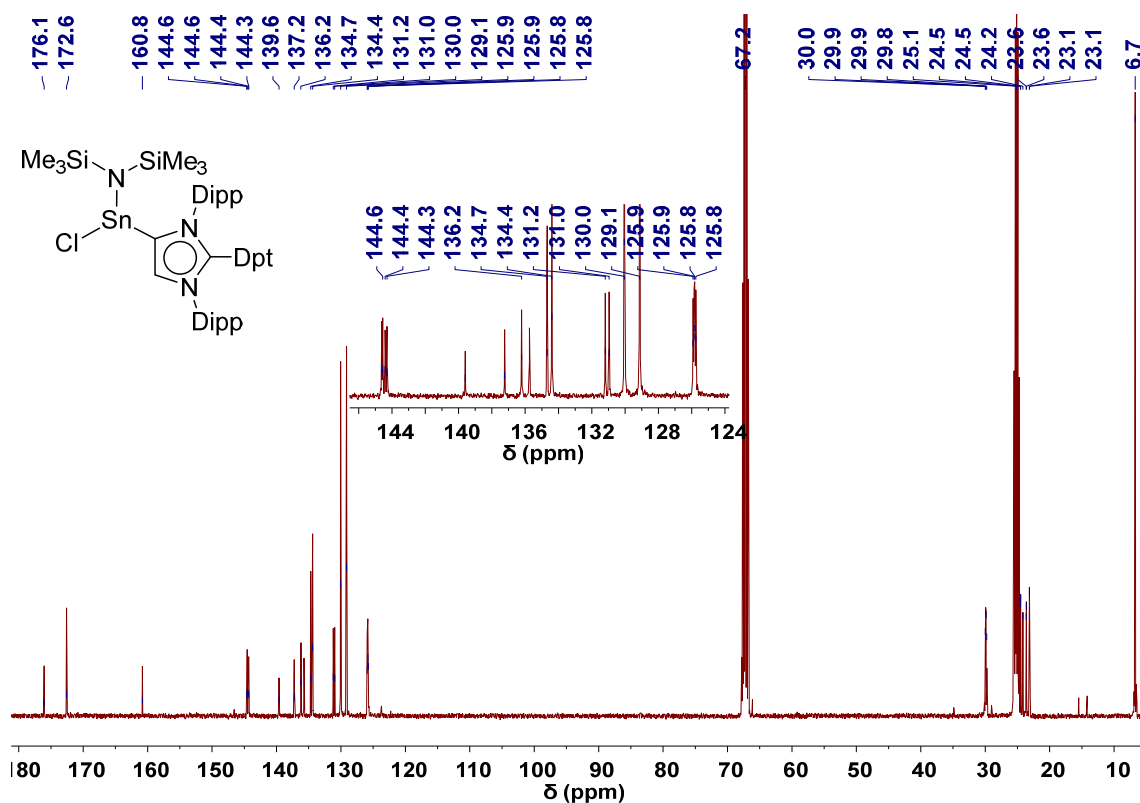


Figure S4b. $^{13}\text{C}\{^1\text{H}\}$ NMR (151 MHz, 298 K, THF- d_8) spectrum of compound 4.

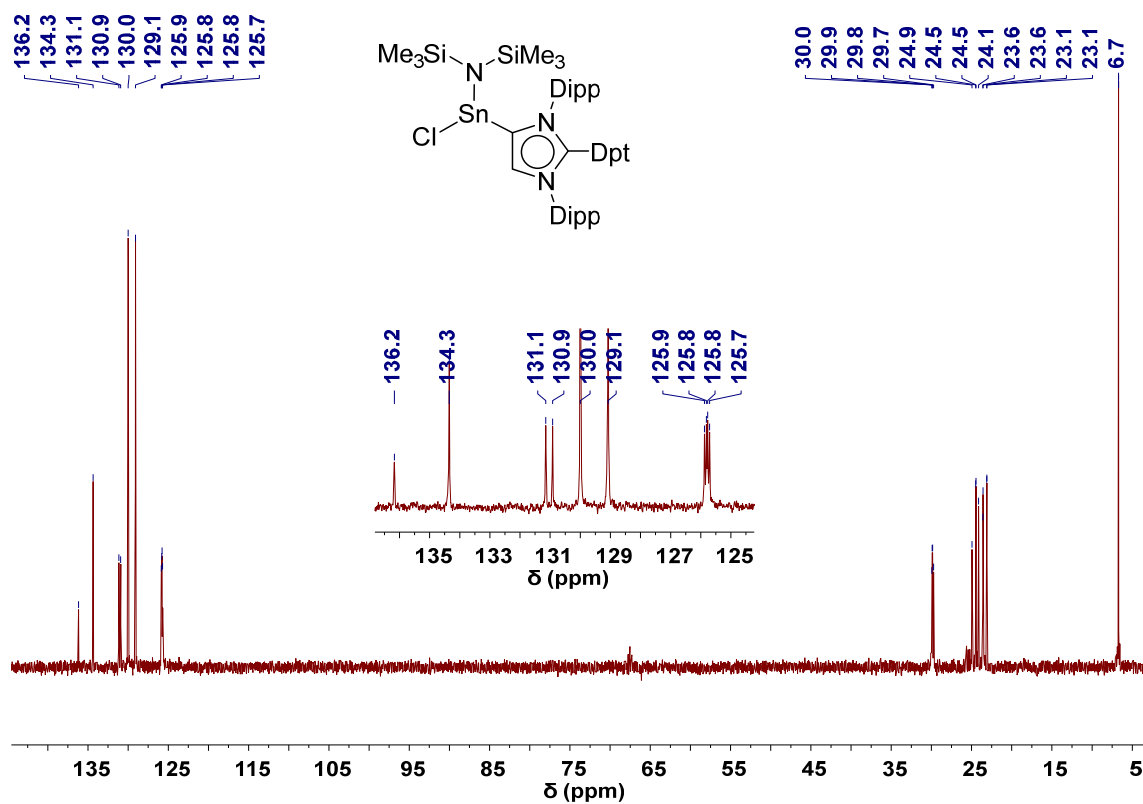


Figure S4c. ^{13}C DEPT NMR (151 MHz, 298 K, THF- d_8) spectrum of compound 4.

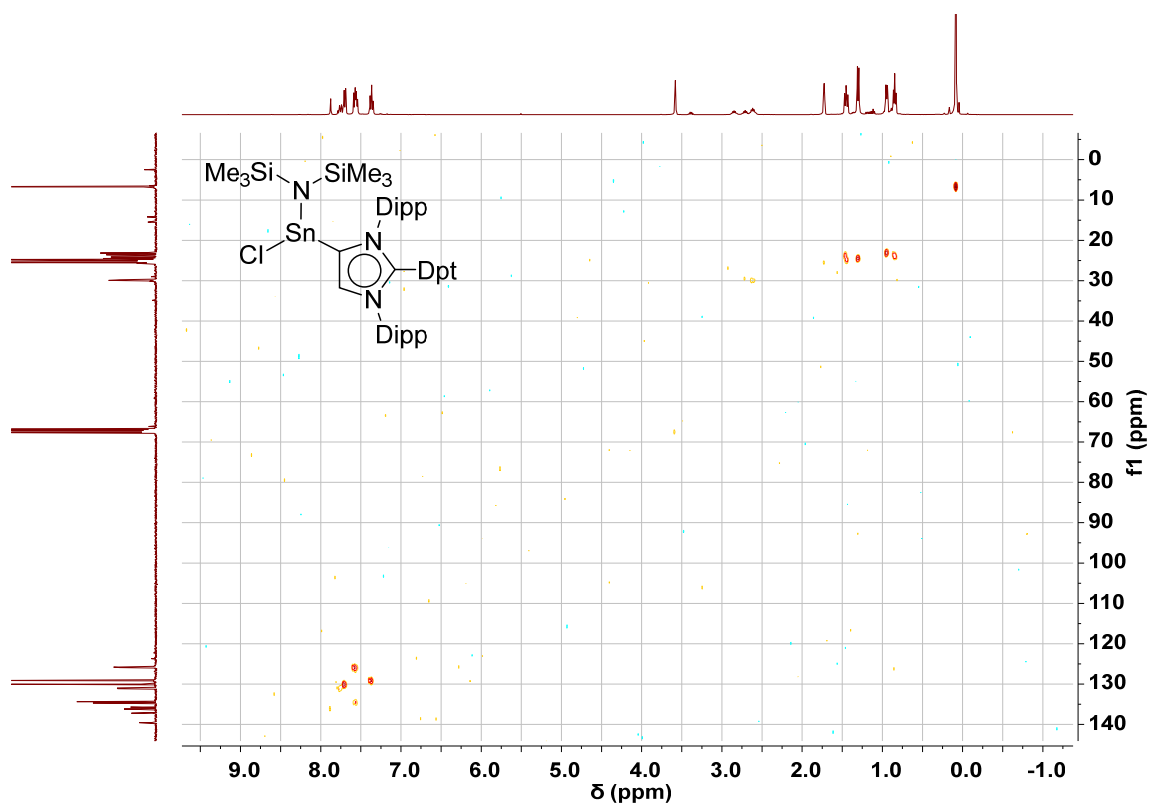
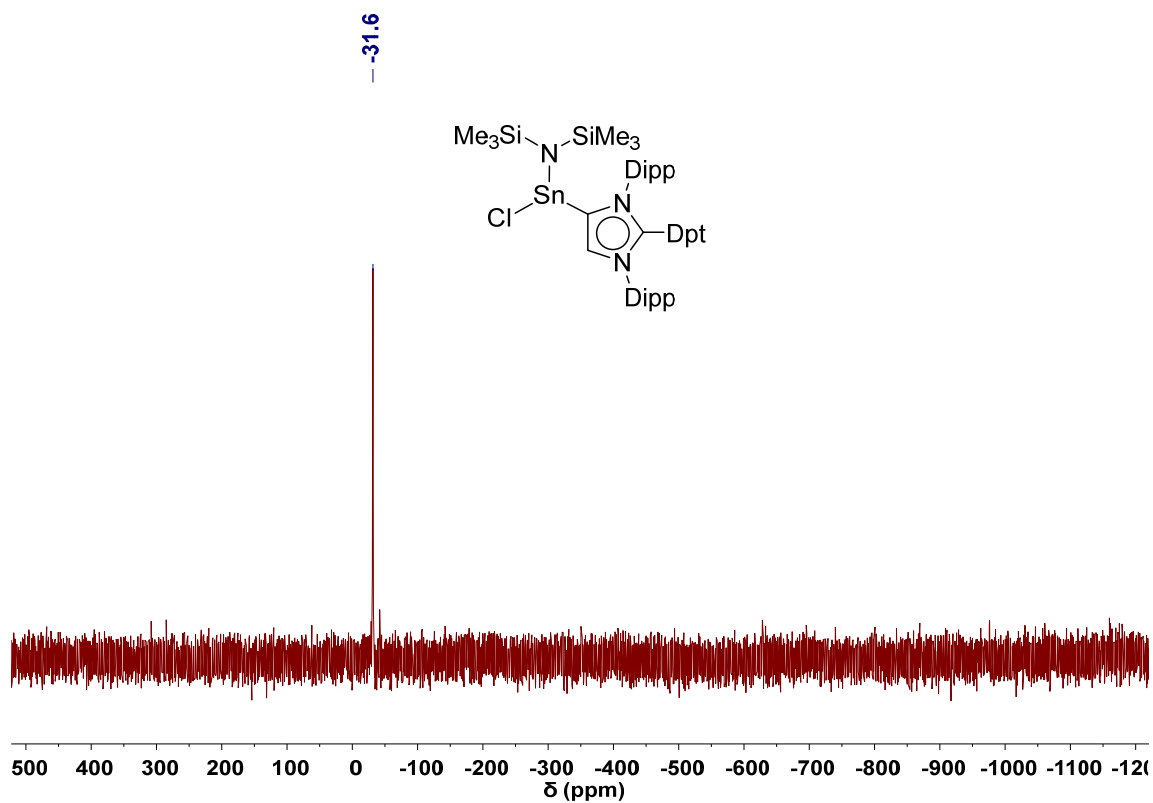
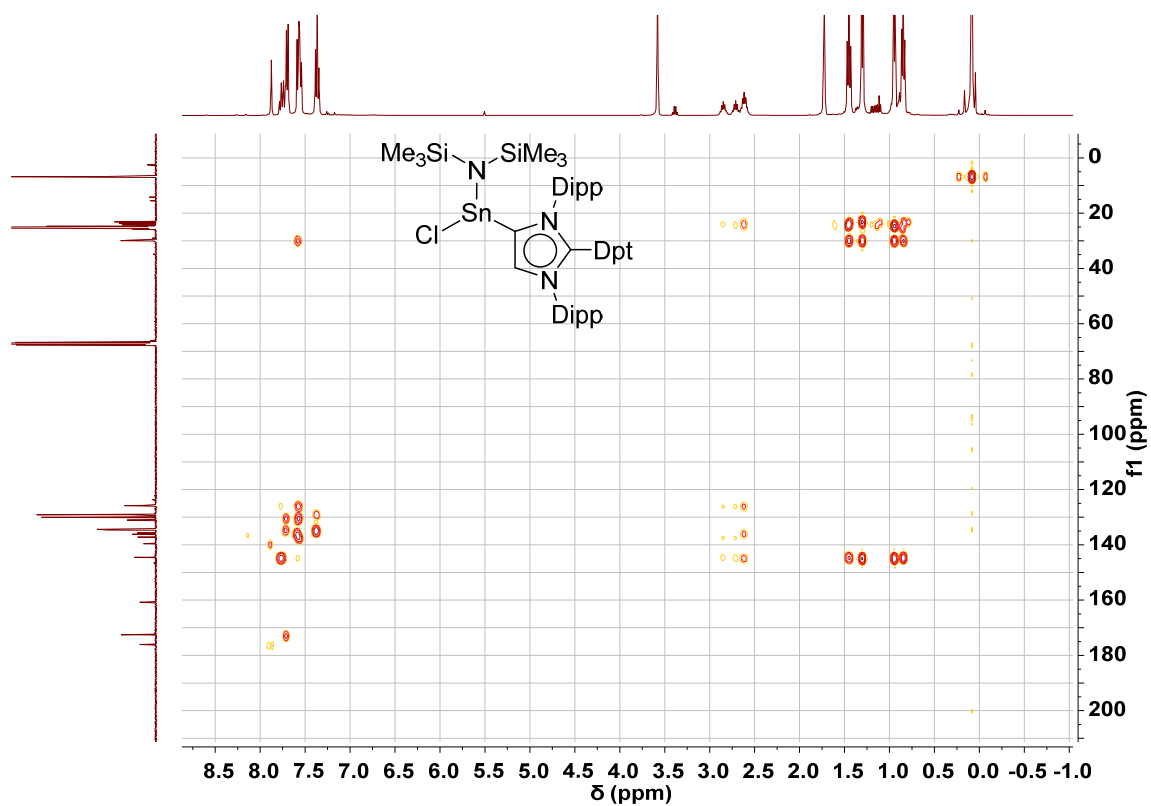
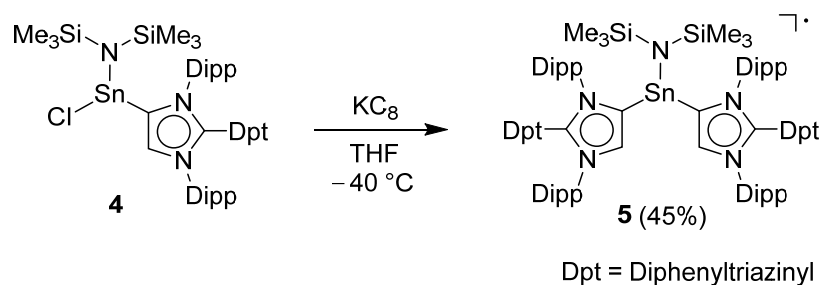


Figure S4d. $^1\text{H}^{13}\text{C}$ HSQC NMR (298 K, THF- d_8) spectrum of compound 4.



Synthesis of neutral radical **5**:



Scheme S5.

KC₈ (14 mg, 0.107 mmol) was added to a stirred THF solution (10 ml) of stannylene **4** (100 mg, 0.107 mmol) at $-40\text{ }^{\circ}\text{C}$. The color of the solution changed immediately to deep purple. The resulting solution was stirred for another 1 h. Subsequently, the solvent was removed under reduced pressure, and the resulting solid was extracted with *n*-pentane/THF (3:1, 15 mL). Then, the deep-purple solution was filtered by using a PTFE syringe filter to remove the KCl and graphite. The filtrate was concentrated to 5 mL and stored at $-40\text{ }^{\circ}\text{C}$ for two days. Purple crystals of neutral radical **5**, suitable for XRD analysis, were obtained (Yield: 37 mg, 45%).

HRMS (nanochip-ESI/LTQ-Orbitrap) m/z : [M]⁺ Calcd for C₉₀H₁₀₈N₁₁Si₂Sn⁺ 1518.7344; Found 1518.7353.

UV-vis (THF solution) [nm]: $\lambda = 400, 505, 546, 593, 653$.

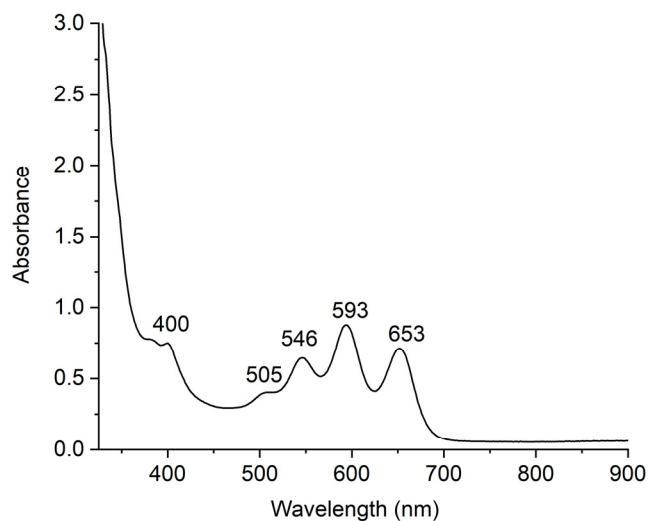
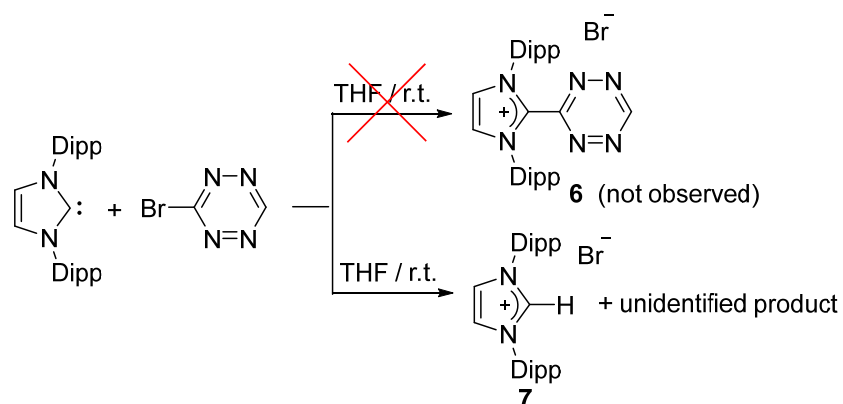


Figure S5. UV-vis spectrum of radical **5** (in THF, 1×10^{-4} M).

Attempt to synthesize the tetrazolyl-substituted imidazolium salt **6**:



Scheme S6.

Synthesis of the tetrazolyl-substituted imidazolium salt **6** was attempted by reaction of IDipp (200 mg, 0.515 mmol) with one equivalent of 3-bromotetrazine (82 mg, 0.515 mmol) in THF (10 mL) at room temperature. The reaction mixture immediately turned to brown, followed by generation of bubbles. After 4 h, formation of a brown precipitate was observed, which was isolated. The solid is insoluble in toluene, THF, DCM, and acetonitrile, but soluble in DMSO. The NMR spectrum in d_6 -DMSO indicates the solid residue is a mixture of imidazolium salt **7** and unidentified byproducts.

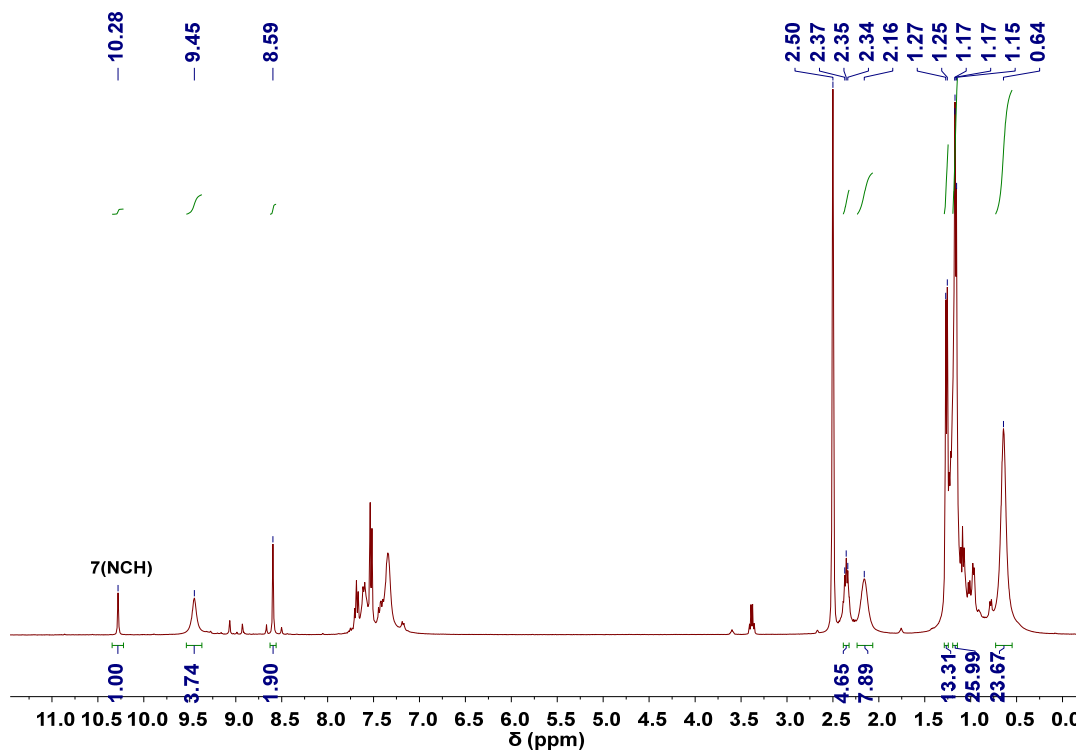


Figure S6. ^1H NMR (400 MHz, 298 K) spectrum of the brown precipitate in d_6 -DMSO.

EPR Measurements

The EPR measurements were performed at room and cryogenic temperatures using a Bruker EleXsys E500 X-band EPR spectrometer (Bruker BioSpin GmbH, Karlsruhe, Germany), which was equipped with a high-Q cylindrical cavity, Model ER 4122 SHQE, and a continuous-flow Helium-gas cryostat, model ESR900, from Oxford Instruments (Abington, UK).

The instrumental settings were: sweep width 150 G; magnetic field modulation frequency 100 kHz; magnetic field modulation amplitude 0.25 G; typical microwave frequency ~ 9.395 GHz; microwave power 0.63 mW and 0.063 mW at 290K and 10 K, respectively; lock-in time constant 10.24 ms; lock-in integration time 40.96 ms; gain 60 dB and 40 dB at 290K and 10 K, respectively; number of points per scan (resolution) 4096; resulting sweeping time 167.7 sec; per each spectrum two scans were accumulated.

The magnetic field strength was calibrated with using a small speck of a solid 2,2'-diphenyl-1-picrylhydrazyl (DPPH) from Sigma-Aldrich. To simulate EPR spectra we employed the public EPR software tool, Win Sim 2002

(<http://www.niehs.nih.gov/research/resources/software/tox-pharm/tools/>).

The EPR spectrum acquired at room temperature ($T = 290$ K) for radical **5** dissolved in THF and its simulation are shown in Figure S7. The g -factor value for radical **5** is of 2.0034. The comparison of the EPR spectra acquired for radical **5** dissolved in THF at room temperature ($T = 290$ K) and at 10 K is shown in Figure S8.

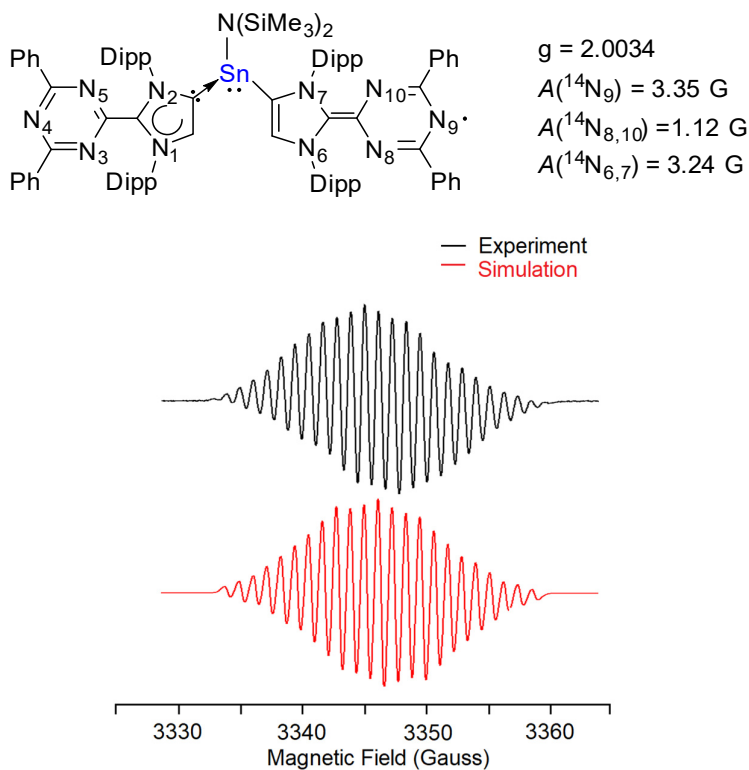


Figure S7. Experimental (top) and simulated (bottom) EPR spectra of radical **5** (in THF solution, $T = 290 \text{ K}$; only one of several possible mesomeric forms of radical **5** is shown).

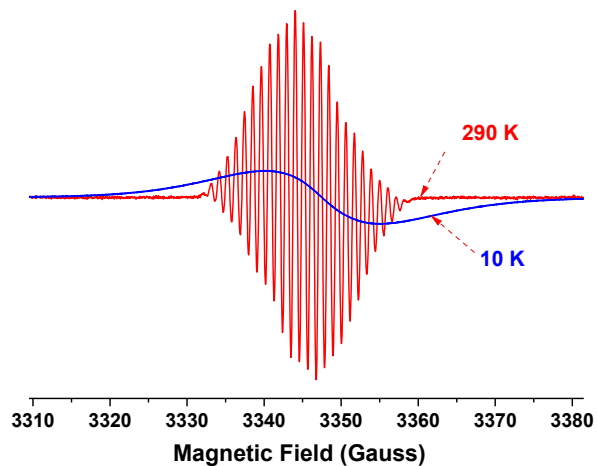


Figure S8. Overlaid EPR spectra acquired for radical **5** (in THF solution) at $T = 290 \text{ K}$ (red trace, $g = 2.0034$) and at $T = 10 \text{ K}$ (blue trace, $g = 2.0035$).

Crystallographic Analyses

Bragg-intensities of **1** – **5** were collected at 140(1) K using $\text{CuK}\alpha$ radiation. . A Rigaku SuperNova dual system diffractometer with an Atlas S2 CCD detector was used for compounds **1**, **2**, **3** and **5**, and one equipped with an Atlas CCD detector for compound **4**. The datasets were reduced and corrected for absorption, with the help of a set of faces enclosing the crystal as snugly as possible, with the latest available version of *CrysAlis^{Pro}*.^[2] The solutions and refinements of the structures were performed by the latest available version of *ShelXT*^[3] and *ShelXL*.^[4] All non-hydrogen atoms were refined anisotropically using full-matrix least-squares based on $|F|^2$. The hydrogen atoms were placed at calculated positions by means of the “riding” model in which each H-atom was assigned a fixed isotropic displacement parameter with a value equal to 1.2 U_{eq} of its parent C-atom (1.5 U_{eq} for the methyl groups). Crystallographic and refinement data are summarized in Table S1. Crystallographic data have been deposited with the Cambridge Crystallographic Data Centre and correspond to the following codes: **1** (2002574), **2** (2064706), **3** (2064707), **4** (2064708) and **5** (2064709). These data can be obtained free of charge via www.ccdc.cam.ac.uk/data_request/cif, or by emailing data_request@ccdc.cam.ac.uk, or by contacting The Cambridge Crystallographic Data Centre, 12 Union Road, Cambridge CB2 1EZ, UK; fax: +44 1223 336033.

Table S1. Crystal data and structure refinement for compounds **1** – **3**.

| Compound | 1 | 2 | 3 |
|---|---|--|---|
| Empirical formula | C ₄₂ H ₄₆ ClN ₅ | C ₄₄ H ₄₅ ClN ₅ O ₂ Rh | C ₄₂ H ₄₅ N ₅ Se |
| Temperature (K) | 140(10) | 140(10) | 140(10) |
| Formula weight | 656.29 | 814.21 | 698.79 |
| Wavelength (Å) | 1.54184 | 1.54184 | 1.54184 |
| Crystal system | monoclinic | orthorhombic | monoclinic |
| Space group | <i>P2₁/n</i> | <i>Pbca</i> | <i>P2₁/c</i> |
| <i>a</i> (Å) | 16.68116(14) | 23.4076(4) | 19.5001(3) |
| <i>b</i> (Å) | 11.13021(8) | 15.1981(3) | 12.59635(19) |
| <i>c</i> (Å) | 49.9098(3) | 25.1192(5) | 15.8206(3) |
| α (deg) | 90 | 90 | 90 |
| β (deg) | 98.0573(7) | 90 | 109.9657(17) |
| γ (deg) | 90 | 90 | 90 |
| <i>V</i> (Å ³) | 9175.03(12) | 8936.2(3) | 3652.45(10) |
| <i>Z</i> | 8 | 8 | 4 |
| <i>D</i> _{calcd} (Mg / m ³) | 0.950 | 1.210 | 1.271 |
| μ (mm ⁻¹) | 0.951 | 3.939 | 1.661 |
| <i>F</i> (000) | 2800 | 3376 | 1464 |
| θ range (°) | 3.514 ~ 72.717 | 3.777 ~ 72.741 | 4.259 ~ 72.708 |
| Ref. collected | 71600 | 75154 | 31302 |
| Independent reflections | 17976 (<i>R</i> _{int} = 0.0189) | 8830 (<i>R</i> _{int} = 0.0787) | 7189 (<i>R</i> _{int} = 0.0422) |
| Completeness to θ (°) | 72.72 (99.9 %) | 72.741 (100 %) | 72.708 (100 %) |
| Goodness-of-fit on $ F ^2$ | 1.029 | 1.064 | 1.024 |
| Final <i>R</i> indices [<i>I</i> > 2 σ (<i>I</i>)] ^a | <i>R</i> ₁ = 0.0590 <i>wR</i> ₂ = 0.1690 | <i>R</i> ₁ = 0.0640 <i>wR</i> ₂ = 0.0724 | <i>R</i> ₁ = 0.0389 <i>wR</i> ₂ = 0.0527 |
| <i>R</i> indices (all data) | <i>R</i> ₁ = 0.0645 <i>wR</i> ₂ = 0.1739 | <i>R</i> ₁ = 0.1693 <i>wR</i> ₂ = 0.1773 | <i>R</i> ₁ = 0.0954 <i>wR</i> ₂ = 0.1031 |
| $\Delta\rho_{\max, \min}$ (e/Å ³) | 0.819, -0.333 | 1.601, -1.211 | 0.610, -0.670 |
| CCDC | 2002574 | 2064706 | 2064707 |

^a $R_1 = \frac{\sum |F_o| - \sum |F_c|}{\sum |F_o|}$, $wR_2 = \frac{[\sum w(F_o^2 - F_c^2)^2 / \sum w(F_o^2)^2]}{1/2}$

Table S2. Crystal data and structure refinement for compounds **4** and **5**.

| Compound | 4 | 5 |
|---|---|---|
| Empirical formula | C ₄₈ H ₆₃ ClN ₆ Si ₂ Sn | C ₉₀ H ₁₀₈ N ₁₁ Si ₂ Sn |
| Temperature (K) | 140(10) | 140(10) |
| Formula weight | 934.36 | 1518.74 |
| Wavelength (Å) | 1.54184 | 1.54184 |
| Crystal system | triclinic | triclinic |
| Space group | $P\bar{1}$ | $P\bar{1}$ |
| <i>a</i> (Å) | 8.9055(4) | 12.5839(3) |
| <i>b</i> (Å) | 12.9674(5) | 19.3739(4) |
| <i>c</i> (Å) | 21.3459(9) | 20.6241(4) |
| α (deg) | 85.945(3) | 112.914(2) |
| β (deg) | 84.773(4) | 94.2721(18) |
| γ (deg) | 88.272(3) | 104.524(2) |
| <i>V</i> (Å ³) | 2447.94(18) | 4399.01(18) |
| <i>Z</i> | 2 | 2 |
| <i>D</i> _{calcd} (Mg / m ³) | 1.268 | 1.147 |
| μ (mm ⁻¹) | 5.407 | 2.937 |
| <i>F</i> (000) | 976 | 1606 |
| θ range (°) | 3.418 ~ 71.792 | 3.698 ~ 72.664 |
| Ref. collected | 9493 | 37366 |
| Independent reflections | 9493 (R _{int} = n/a) | 17061 (R _{int} = 0.0272) |
| Completeness to θ (°) | 71.792 (98.6 %) | 72.664 (99.0 %) |
| Goodness-of-fit on $ F ^2$ | 1.048 | 1.032 |
| Final <i>R</i> indices [<i>I</i> > 2 σ (<i>I</i>)] ^a | <i>R</i> ₁ = 0.0684 <i>wR</i> ₂ = 0.1817 | <i>R</i> ₁ = 0.0284 <i>wR</i> ₂ = 0.0686 |
| <i>R</i> indices (all data) | <i>R</i> ₁ = 0.0914 <i>wR</i> ₂ = 0.1925 | <i>R</i> ₁ = 0.0327 <i>wR</i> ₂ = 0.0707 |
| $\Delta\rho_{\max, \min}$ (e/Å ³) | 2.073, -0.870 | 0.399, -0.550 |
| CCDC | 2064708 | 2064709 |

$$^a R_1 = \frac{\sum |F_o| - |F_c|}{\sum |F_o|}, wR_2 = \left[\frac{\sum w(F_o^2 - F_c^2)^2}{\sum w(F_o^2)^2} \right]^{1/2}$$

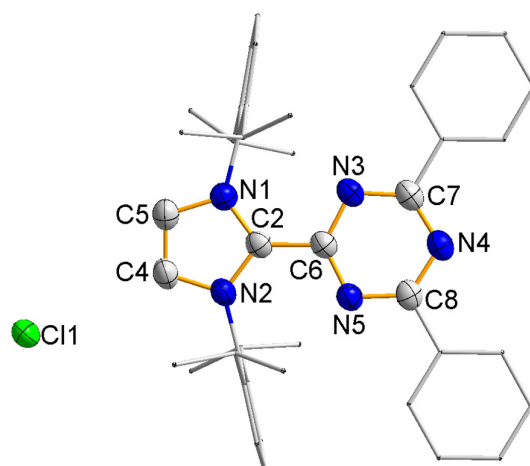


Figure S9. Molecular structure of imidazolium salt **1** in the crystal (thermal ellipsoids at 50% probability; all hydrogen atoms are omitted for clarity; Dipp and phenyl groups are simplified as wireframes). Selected atom distances [Å] and dihedral angles [°]: C2–C6 1.471(2), C4–C5 1.346(3), C2–N1 1.349(2), C2–N2 1.350(2), C6–N3 1.332(2), C6–N5 1.326(2), C7–N3 1.345(2), C8–N5 1.349(2), C7–N4 1.336(3), C8–N4 1.333(2), N1–C2–C6–N5 179.3(17), N2–C2–C6–N3 177.6(17).

N.B.: There are two crystallographically independent molecules in the asymmetric unit. We only give the bond lengths of one of them, but the bond lengths are similar in both molecules.

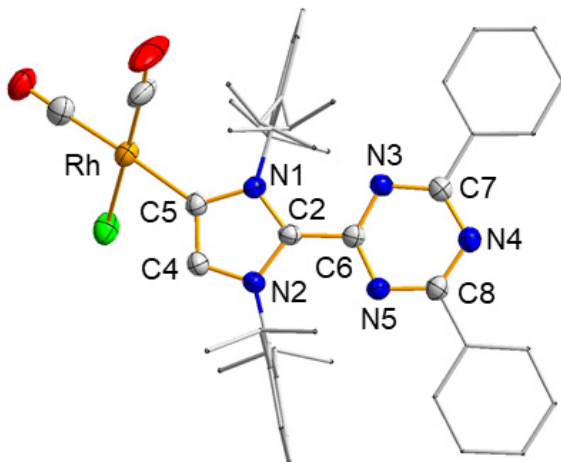


Figure S10. Molecular structure of rhodium complex **2** in the crystal (thermal ellipsoids at 50% probability; all hydrogen atoms are omitted for clarity; Dipp and phenyl groups are simplified as wireframes). Selected atom distances [Å] and dihedral angles [°]: Rh–C5 2.078(4), C2–C6 1.468(5), C4–C5 1.370(5), C2–N1 1.360(4), C2–N2 1.358(4), C6–N3 1.328(4), C6–N5 1.326(4), C7–N3 1.349(4), C8–N5 1.346(5), C7–N4 1.332(5), C8–N4 1.337(5), N1–C2–C6–N5 174.2(3), N2–C2–C6–N3 179.3(3).

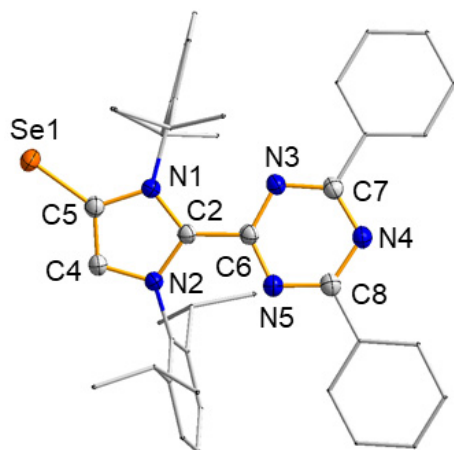


Figure S11. Molecular structure of MIC-Se adduct **3** in the crystal (thermal ellipsoids at 50% probability; all hydrogen atoms are omitted for clarity; Dipp and phenyl groups are simplified as wireframes). Selected atom distances [Å] and dihedral angles [°]: Se–C5 1.857(2), C2–C6 1.459(2), C4–C5 1.375(3), C2–N1 1.362(3), C2–N2 1.359(3), C6–N3 1.333(3), C6–N5 1.334(3), C7–N3 1.343(3), C8–N5 1.340(3), C7–N4 1.338(3), C8–N4 1.340(3), N1–C2–C6–N5 165.9(19), N2–C2–C6–N3 167.1(19).

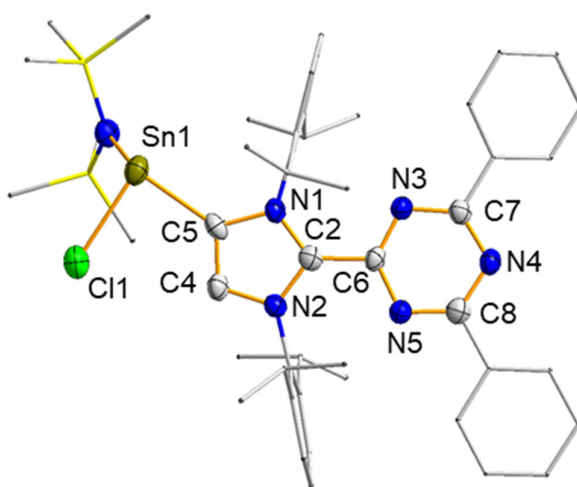


Figure S12. Molecular structure of **4** in the crystal (thermal ellipsoids at 50% probability; all hydrogen atoms are omitted for clarity; Dipp, Me₃Si and phenyl groups are simplified as wireframes). Selected atom distances [Å] and dihedral angles [°]: Sn1–C5 2.295(7), Sn1–Cl1 2.507(18), C2–C6 1.481(8), C4–C5 1.383(9), C2–N1 1.350(8), C2–N2 1.351(8), C6–N3 1.313(8), C6–N5 1.335(8), C7–N3 1.342(5), C8–N5 1.329(8), C7–N4 1.328(8), C8–N4 1.345(8), N1–C2–C6–N5 178.9(5), N2–C2–C6–N3 172.3(5).

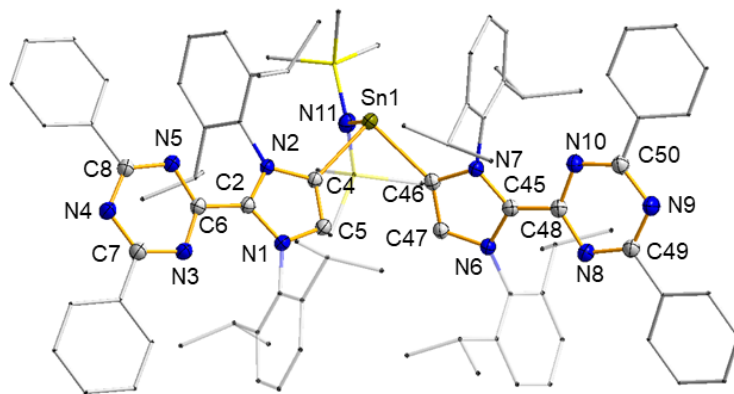


Figure S13. Molecular structure of radical **5** in the crystal (thermal ellipsoids at 50% probability; all hydrogen atoms are omitted for clarity; Dipp, Me₃Si and phenyl groups are simplified as wireframes). Selected atom distances [Å] and dihedral angles [°]: Sn1–C4 2.300(16), Sn1–C46 2.293(16), Sn1–N11 2.160(13), C2–C6 1.476(2), C4–C5 1.368(2), C2–N1 1.346(2), C2–N2 1.357(2), C6–N3 1.327(2), C6–N5 1.329(2), C7–N3 1.352(2), C8–N5 1.345(2), C7–N4 1.408(2), C8–N4 1.336(2), C45–C48 1.420(2), C46–C47 1.356(2), C45–N6 1.370(2), C45–N7 1.378(2), C48–N8 1.370(2), C48–N10 1.378(2), C49–N8 1.326(2), C50–N10 1.318(2), C49–N9 1.355(2), C50–N9 1.353(2), N1–C2–C6–N5 172.2(14), N2–C2–C6–N3 168.4(15), N6–C45–C48–N10 174.1(15), N7–C45–C48–N8 173.4(14).

Table S3. Comparison of structural parameters of compounds **1–5** (bond lengths in Å; dihedral angles in °).

| | 1 | 2 | 3 | 4 | 5 |
|---|----------|----------|----------|----------|-----------|
| N1–C2 | 1.349(2) | 1.360(4) | 1.362(3) | 1.350(8) | 1.346(2) |
| N2–C2 | 1.350(2) | 1.358(4) | 1.359(3) | 1.351(8) | 1.357(2) |
| C2–C6 | 1.471(2) | 1.468(5) | 1.459(2) | 1.481(8) | 1.476(2) |
| C4–C5 | 1.346(3) | 1.370(5) | 1.375(3) | 1.383(9) | 1.368(2) |
| N3–C6 | 1.332(2) | 1.328(4) | 1.333(3) | 1.313(8) | 1.327(2) |
| N3–C7 | 1.345(2) | 1.349(4) | 1.343(3) | 1.342(5) | 1.352(2) |
| N4–C7 | 1.336(3) | 1.332(5) | 1.338(3) | 1.328(8) | 1.408(2) |
| N4–C8 | 1.333(2) | 1.337(5) | 1.340(3) | 1.345(8) | 1.336(2) |
| N5–C6 | 1.326(2) | 1.326(4) | 1.334(3) | 1.335(8) | 1.329(2) |
| N5–C8 | 1.349(2) | 1.346(5) | 1.340(3) | 1.329(8) | 1.345(2) |
| α (C ₃ N ₂ /C ₃ N ₃) ^a | 4.7 | 8.0 | 12.8 | 8.2 | 9.7 / 6.3 |

a: The angle α is defined as the dihedral angle between the plane of the imidazole ring (C₃N₂) and the plane of the triazinyl ring (C₃N₃).

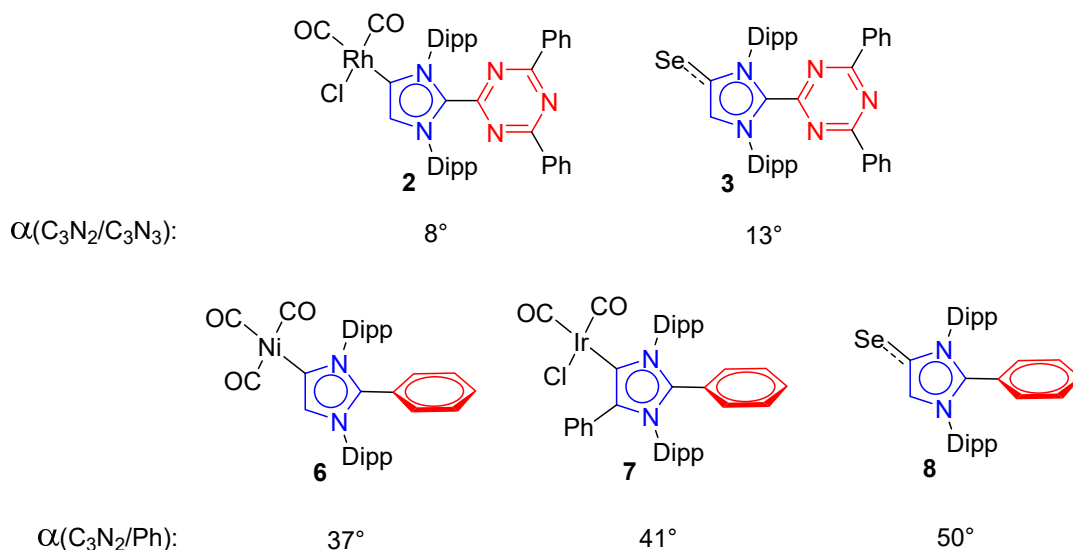


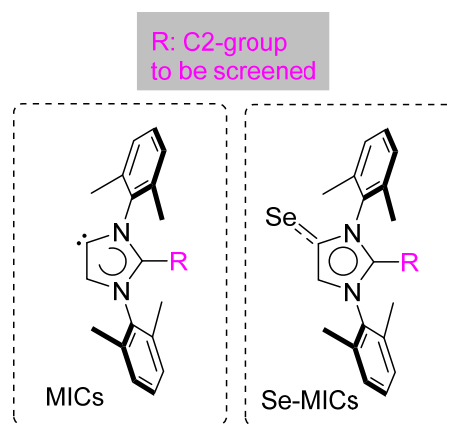
Figure S14. The dihedral angle between the plane of the imidazole ring (C₃N₂) and the plane of the triazinyl ring (C₃N₃) of Dpt-MIC complexes **2–3**, and the dihedral angle between the plane of the imidazole ring (C₃N₂) and the plane of the phenyl ring (Ph) of the reported Ph-MIC complexes **6–8**.^[5]

Computational Details

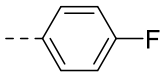
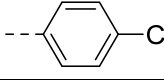
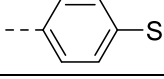

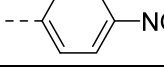
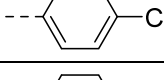
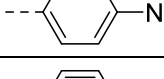
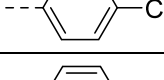

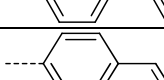
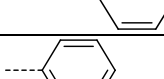
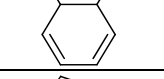
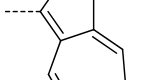
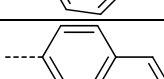
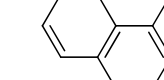
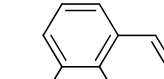
All DFT computations were carried out using the Gaussian16 package (revision A.03).^[6] Gas phase geometry optimizations of free carbenes (MIC1—MIC71) and Se adducts (Se-MIC1—Se-MIC71) were performed using the PBE0 functional^[7] with D3BJ dispersion correction^[8] and the def2-SVP basis set for all atoms.^[9] Frequency computations confirmed that all optimized molecular geometries were minima. Isotropic ⁷⁷Se shifts were computed using the ‘NMR’ keyword and the default Gauge-Independent Atomic Orbital (GIAO) method^[10], with the same functional and the def2-TZVPP basis set for all atoms. Reported chemical shifts were obtained by subtracting the isotropic shift of the Se adduct from that of a dimethylselenide standard. Dimethylselenide was optimized and its NMR shift were computed at the same level as the Se adducts (PBE0/def2-TZVPP//PBE0(D3BJ)/def2-SVP).

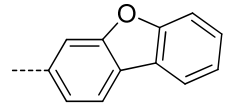
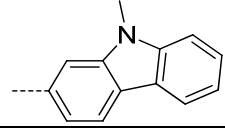
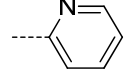
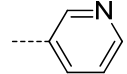
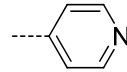
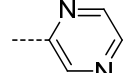
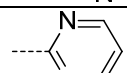
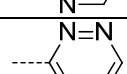
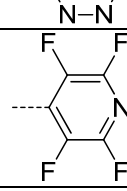
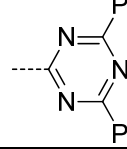
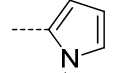
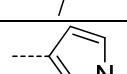
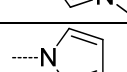
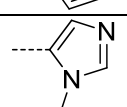
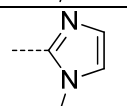
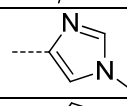
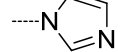
The NBO analyses^[11] were performed with the Version 3.1 of the NBO program which was implemented in the G16 A.03 version of the Gaussian program.^[12] The molecular structure optimization of **5** was performed using the (U)M06-2X functional.^[13] The small 6-31G(d,p) basis set for Si, N, C, H^[14] and the def2-tzvp basis set for Sn were used. In the case of the element Sn, the latter was applied in connection with the corresponding effective core potentials.^[9,15] Stationary points were verified as minima by subsequent frequency calculations (Number of imaginary frequencies (NIMAG): 0).

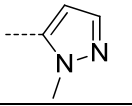
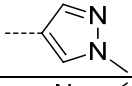
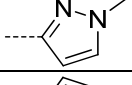
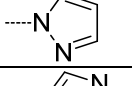
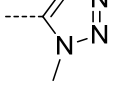
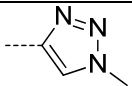
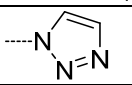
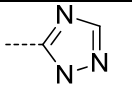
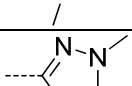
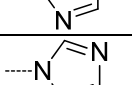
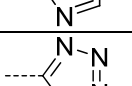
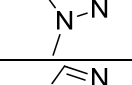
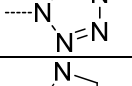
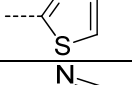
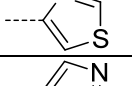
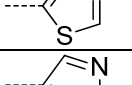
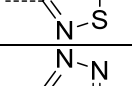
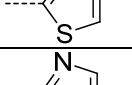
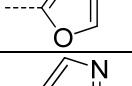
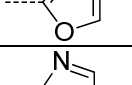
Table S4. Calculated HOMO, LUMO energies of MICs, and ⁷⁷Se NMR chemical shifts of the relevant Se-MIC adducts (all geometry optimizations were performed at PBE0(D3BJ)/def2-SVP level of theory).

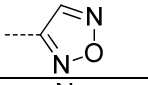
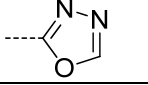
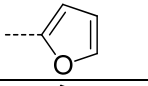
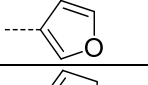
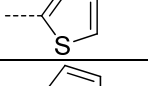
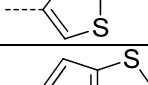
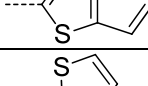
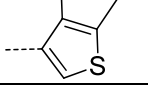
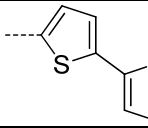
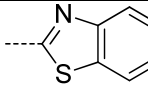
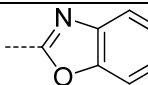
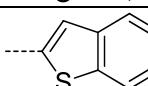
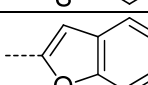
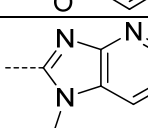
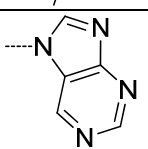
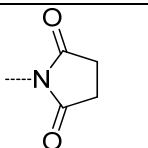


| Index | Structure | HOMO (eV) | LUMO (eV) | Index | ⁷⁷ Se NMR (ppm) |
|-------|-----------|-----------|-----------|---------|----------------------------|
| MIC1 | | -5.11 | -1.24 | Se-MIC1 | -9 |
| MIC2 | | -5.06 | -1.16 | Se-MIC2 | -19 |

| | | | | | |
|-------|---|-------|-------|----------|-----|
| MIC3 |  | -5.17 | -1.24 | Se-MIC3 | -13 |
| MIC4 |  | -5.20 | -1.43 | Se-MIC4 | 5 |
| MIC5 |  | -5.06 | -1.20 | Se-MIC5 | -17 |
| MIC6 |  | -5.00 | -0.97 | Se-MIC6 | -35 |
| MIC7 |  | -5.48 | -2.65 | Se-MIC7 | 148 |
| MIC8 |  | -5.43 | -2.15 | Se-MIC8 | 90 |
| MIC9 |  | -5.37 | -1.98 | Se-MIC9 | 53 |
| MIC10 |  | -5.31 | -1.73 | Se-MIC10 | 39 |
| MIC11 |  | -4.85 | -0.76 | Se-MIC11 | -51 |
| MIC12 |  | -5.11 | -1.56 | Se-MIC12 | 0 |
| MIC13 |  | -5.11 | -1.65 | Se-MIC13 | 5 |
| MIC14 |  | -5.08 | -1.68 | Se-MIC14 | 25 |
| MIC15 |  | -4.96 | -2.42 | Se-MIC15 | -3 |
| MIC16 |  | -5.08 | -2.07 | Se-MIC16 | 50 |
| MIC17 |  | -5.08 | -2.04 | Se-MIC17 | -11 |
| MIC18 |  | -5.12 | -1.90 | Se-MIC18 | 4 |

| | | | | | |
|-------|---|----------|----------|----------|-----|
| MIC19 |  | -5.13 | -1.68 | Se-MIC19 | 7 |
| MIC20 |  | -5.08 | -1.48 | Se-MIC20 | -12 |
| MIC21 |  | -5.09 | -1.52 | Se-MIC21 | 32 |
| MIC22 |  | -5.23 | -1.49 | Se-MIC22 | 14 |
| MIC23 |  | -5.34 | -1.69 | Se-MIC23 | 50 |
| MIC24 |  | -5.25 | -1.92 | Se-MIC24 | 81 |
| MIC25 |  | -5.17642 | -1.79078 | Se-MIC25 | 111 |
| MIC26 |  | -5.54 | -3.05 | Se-MIC26 | 270 |
| MIC27 |  | -5.52 | -2.10 | Se-MIC27 | 99 |
| MIC28 |  | -5.41 | -2.23 | Se-MIC28 | 218 |
| MIC29 |  | -5.06 | -0.77 | Se-MIC29 | -3 |
| MIC30 |  | -4.85 | -0.58 | Se-MIC30 | -74 |
| MIC31 |  | -5.19 | -0.78 | Se-MIC31 | -50 |
| MIC32 |  | -5.16 | -1.00 | Se-MIC32 | -28 |
| MIC33 |  | -5.18 | -0.84 | Se-MIC33 | 3 |
| MIC34 |  | -4.84 | -0.67 | Se-MIC34 | -45 |
| MIC35 |  | -5.36 | -0.92 | Se-MIC35 | -37 |

| | | | | | |
|-------|---|-------|-------|----------|-----|
| MIC36 |  | -5.23 | -1.06 | Se-MIC36 | -17 |
| MIC37 |  | -5.01 | -0.75 | Se-MIC37 | -65 |
| MIC38 |  | -4.97 | -0.71 | Se-MIC38 | -54 |
| MIC39 |  | -5.26 | -0.74 | Se-MIC39 | -40 |
| MIC40 |  | -5.44 | -1.30 | Se-MIC40 | 42 |
| MIC41 |  | -5.03 | -0.89 | Se-MIC41 | -24 |
| MIC42 |  | -5.45 | -1.14 | Se-MIC42 | -17 |
| MIC43 |  | -5.28 | -1.08 | Se-MIC43 | -5 |
| MIC44 |  | -4.99 | -0.75 | Se-MIC44 | -33 |
| MIC45 |  | -5.44 | -1.00 | Se-MIC45 | -22 |
| MIC46 |  | -5.48 | -1.40 | Se-MIC46 | 29 |
| MIC47 |  | -5.66 | -1.45 | Se-MIC47 | 3 |
| MIC48 |  | -5.31 | -1.74 | Se-MIC48 | 54 |
| MIC49 |  | -5.10 | -1.40 | Se-MIC49 | 2 |
| MIC50 |  | -5.29 | -1.65 | Se-MIC50 | 20 |
| MIC51 |  | -5.40 | -2.02 | Se-MIC51 | 61 |
| MIC52 |  | -5.49 | -1.99 | Se-MIC52 | 104 |
| MIC53 |  | -5.26 | -1.36 | Se-MIC53 | 52 |
| MIC54 |  | -5.33 | -1.42 | Se-MIC54 | 2 |
| MIC55 |  | -5.12 | -1.06 | Se-MIC55 | -7 |

| | | | | | |
|-------|---|-------|-------|----------|-----|
| MIC56 |  | -5.54 | -1.88 | Se-MIC56 | 50 |
| MIC57 |  | -5.46 | -1.62 | Se-MIC57 | 92 |
| MIC58 |  | -5.16 | -1.15 | Se-MIC58 | -24 |
| MIC59 |  | -5.11 | -0.88 | Se-MIC59 | -46 |
| MIC60 |  | -5.15 | -1.39 | Se-MIC60 | -9 |
| MIC61 |  | -5.12 | -1.16 | Se-MIC61 | -23 |
| MIC62 |  | -5.19 | -1.64 | Se-MIC62 | 11 |
| MIC63 |  | -5.13 | -1.33 | Se-MIC63 | -12 |
| MIC64 |  | -5.19 | -1.88 | Se-MIC64 | 31 |
| MIC65 |  | -5.38 | -1.94 | Se-MIC65 | 103 |
| MIC66 |  | -5.36 | -1.81 | Se-MIC66 | 141 |
| MIC67 |  | -5.23 | -1.66 | Se-MIC67 | 32 |
| MIC68 |  | -5.27 | -1.60 | Se-MIC68 | 27 |
| MIC69 |  | -5.42 | -1.91 | Se-MIC69 | 61 |
| MIC70 |  | -5.57 | -1.69 | Se-MIC70 | 14 |
| MIC71 |  | -5.21 | -1.11 | Se-MIC71 | -41 |

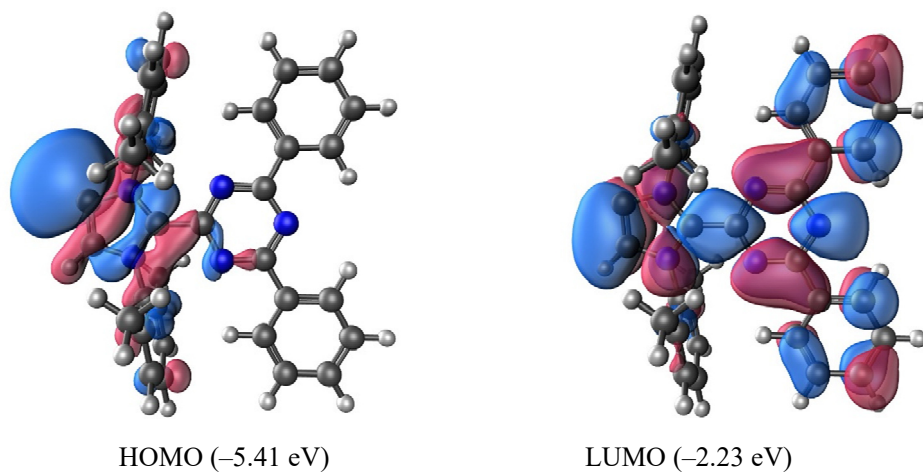


Figure S15. Selected surface diagrams of the frontier orbitals of Dpt-MIC (at an isodensity value of 0.04). Color code: blue, nitrogen; gray, carbon; hydrogen, white.

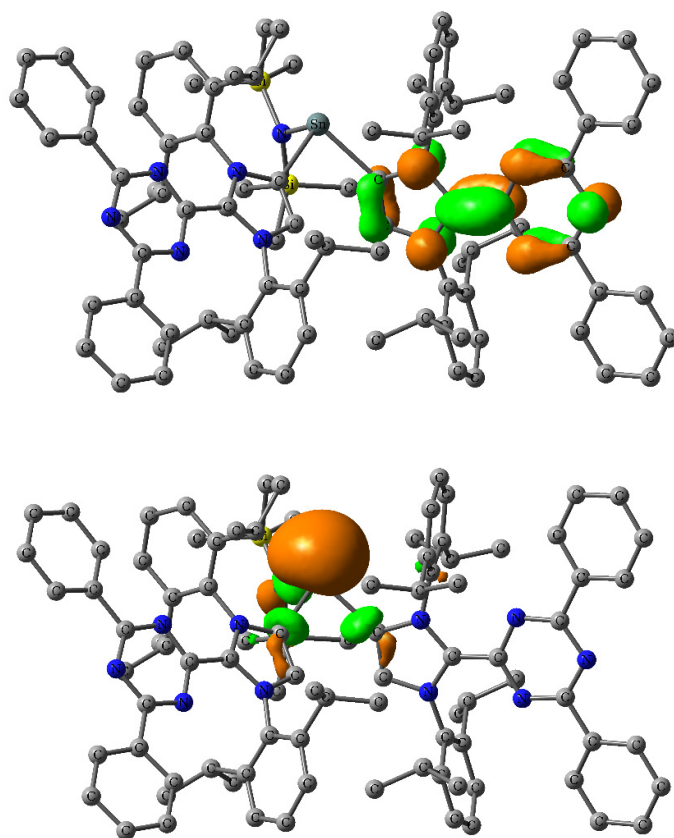


Figure S16. Surface diagrams of SOMO (top) and HOMO(α) (bottom) of radical **5** (isovalue = 0.05; calculated at the UM06-2X/6-31(d,p)(H,C,N,Si), def2-tzvp(Sn) level). Color code: blue, nitrogen; gray, carbon; hydrogen atoms are omitted for clarity.

References

- [1] X. Bantril, S. P. Nolan, *Nat. Protoc.* **2011**, *6*, 69–77.
- [2] *CrysAlis^{Pro}*, Rigaku Oxford Diffraction, **2020**.
- [3] G. M. Sheldrick, *Acta Crystallogr. Sect. A* **2015**, *71*, 3–8.
- [4] G. M. Sheldrick, *Acta Crystallogr. Sect. C* **2015**, *71*, 3–8.
- [5] (a) A. Merschel, D. Rottschäfer, B. Neumann, H. G. Stammer, R. S. Ghadwal, *Organometallics* **2020**, *39*, 1719–1729; (b) G. Ung, G. Bertrand, *Chem. Eur. J.* **2011**, *17*, 8269–8272
- [6] M. J. Frisch, G. W. Trucks, H. B. Schlegel, G. E. Scuseria, M. A. Robb, J. R. Cheeseman, G. Scalmani, V. Barone, G. A. Petersson, H. Nakatsuji, X. Li, M. Caricato, A. V. Marenich, J. Bloino, B. G. Janesko, R. Gomperts, B. Mennucci, H. P. Hratchian, J. V. Ortiz, A. F. Izmaylov, J. L. Sonnenberg, D. Williams-Young, F. Ding, F. Lipparini, F. Egidi, J. Goings, B. Peng, A. Petrone, T. Henderson, D. Ranasinghe, V. G. Zakrzewski, J. Gao, N. Rega, G. Zheng, W. Liang, M. Hada, M. Ehara, K. Toyota, R. Fukuda, J. Hasegawa, M. Ishida, T. Nakajima, Y. Honda, O. Kitao, H. Nakai, T. Vreven, K. Throssell, J. A. Montgomery, Jr., J. E. Peralta, F. Ogliaro, M. J. Bearpark, J. J. Heyd, E. N. Brothers, K. N. Kudin, V. N. Staroverov, T. A. Keith, R. Kobayashi, J. Normand, K. Raghavachari, A. P. Rendell, J. C. Burant, S. S. Iyengar, J. Tomasi, M. Cossi, J. M. Millam, M. Klene, C. Adamo, R. Cammi, J. W. Ochterski, R. L. Martin, K. Morokuma, O. Farkas, J. B. Foresman, and D. J. Fox, Gaussian16, Revision A. 03, Inc. Wallingford CT, **2016**.
- [7] (a) J. P. Perdew, K. Burke, M. Ernzerhof, *Phys. Rev. Lett.*, **1996**, *77*, 3865–3868; (b) C. Adamo, V. Barone, *J. Chem. Phys.* **1999**, *110*, 6158–6170.
- [8] (a) S. Grimme, J. Antony, S. Ehrlich, H. Krieg, *J. Chem. Phys.*, **2010**, *132*, 154104; (b) S. Grimme, S. Ehrlich, L. Goerigk, *J. Comput. Chem.* **2011**, *32*, 1456–1465.
- [9] F. Weigend, R. Ahlrichs, *Phys. Chem. Chem. Phys.* **2005**, *7*, 3297–3305.
- [10] (a) R. Ditchfield, *Mol. Phys.* **1974**, *27*, 789–807; (b) K. Wolinski, J. F. Hinton, P. Pulay, *J. Am. Chem. Soc.* **1990**, *112*, 8251–8260.
- [11] A. E. Reed, L. A. Curtiss, F. Weinhold, *Chem. Rev.* **1988**, *88*, 899–926.
- [12] NBO Version 3.1, E. D. Glendening, A. E. Reed, J. E. Carpenter, F. Weinhold.
- [13] Y. Zhao, N. E. Schultz, D. G. Truhlar, *J. Chem. Theory Comput.* **2006**, *2*, 364–382.
- [14] (a) R. Ditchfield, W. J. Hehre, J. Pople, *J. Chem. Phys.* **1971**, *54*, 724–728; (b) W. J. Hehre, R. Ditchfield, J. A. Pople, *J. Chem. Phys.* **1972**, *56*, 2257–2261; (c) P. C. Hariharan, J. A. Pople, *Theor. Chem. Acc.* **1973**, *28*, 213–222.
- [15] (a) D. Andrae, U. Haeussermann, M. Dolg, H. Stoll, H. Preuss, *Theor. Chim. Acta.* **1990**, *77*, 123–141; (b) B. Metz, H. Stoll, M. Dolg, *J. Chem. Phys.* **2000**, *113*, 2563–2569.